

2018 Fall

“Phase Transformation *in* Materials”

10.25.2018

Eun Soo Park

Office: 33-313

Telephone: 880-7221

Email: espark@snu.ac.kr

Office hours: by an appointment

Summary for today's class

- **Thermally Activated Migration of Grain Boundaries:**

Metastable equilibrium of grain boundary (Balances of 1) boundary E + 2) surface tension)

→ real curvature ($\Delta P \rightarrow \Delta G$: Gibbs Thomson Eq.) → $F = 2\gamma/r = \Delta G/V_m$ (by curvature)

(Pulling force per unit area of boundary)

→ Grain coarsening at high T annealing

- **Kinetics of Grain Growth**

- Grain boundary migration (v) by thermally activated atomic jump

Boundary velocity $v = \frac{A_2 n_1 v_1 V_m^2}{N_a RT} \exp\left(-\frac{\Delta G^a}{RT}\right) \frac{\Delta G}{V_m}$

$v \sim \Delta G/V_m$ driving force
→ $F = \Delta G/V_m$

M : mobility = velocity under unit driving force $\sim \exp(-1/T)$

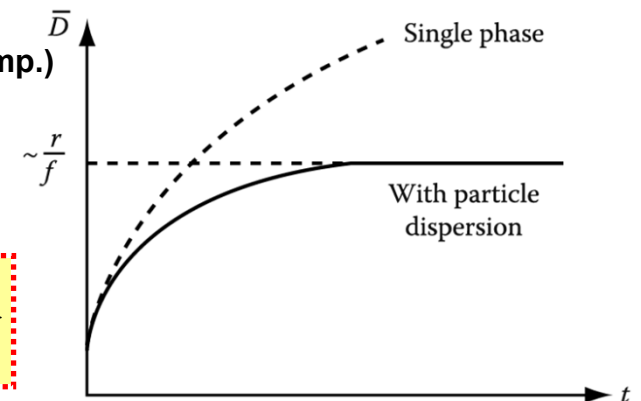
rate of grain growth $d\bar{D}/dt \sim 1/\bar{D}$, exponentially increase with T

→ $\bar{D} = k't^n$ (Experimental: $n \ll 1/2$, $1/2$ at pure metals or high Temp.)

- Mobility of GB ~ affected by both type of boundaries and GB segregation or 2nd phase precipitation

Ex) Effect of second-phase particle - Zener Pinning

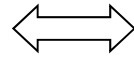
$$\bar{D}_{\max} = \frac{4r}{3f_v}$$



Summary for today's class

- Grain Growth**

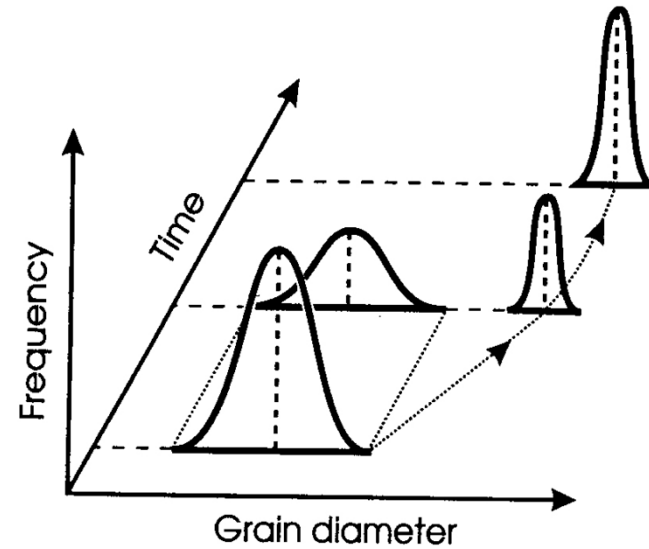
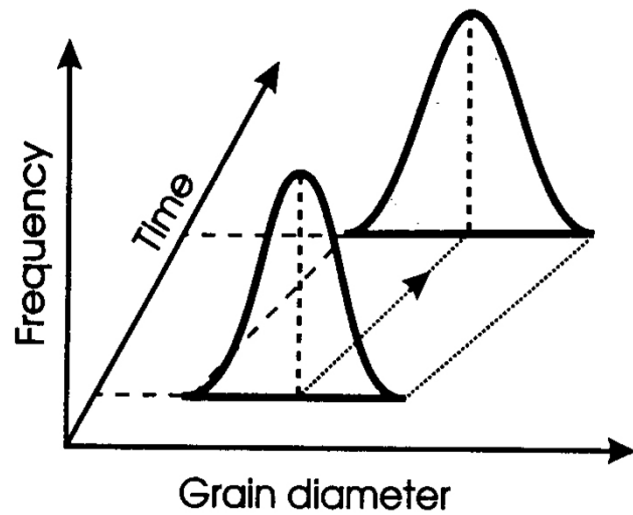
- Normal grain growth



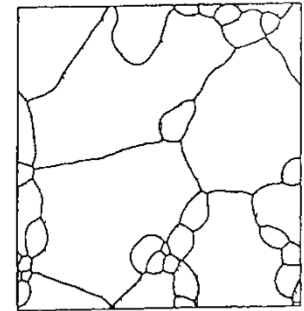
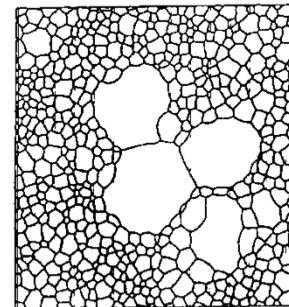
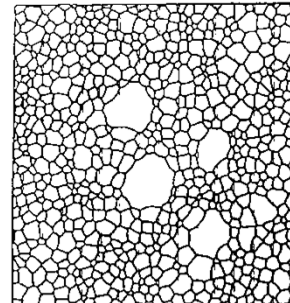
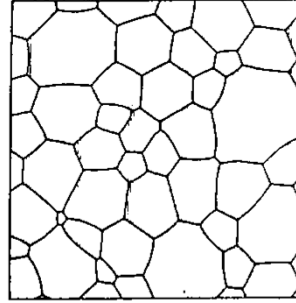
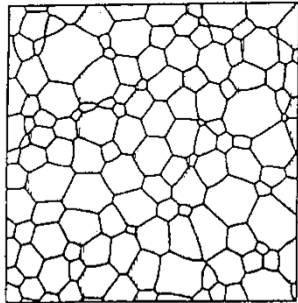
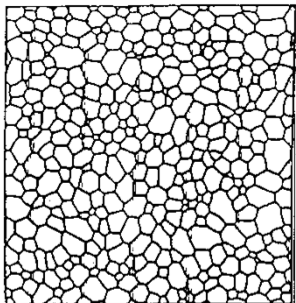
Abnormal grain growth

(high mobility of special GBs

→ development of recrystallization textures)



< Bimodal Size distribution >



Contents for today's class

- **Interphase Interfaces in Solid (α/β)**

- Types of interphase interfaces in solid (α/β)

- **Second-Phase Shape** { **Interface Energy Effects**
Coherent / Semi-coherent / incoherent
Misfit Strain Effects

$$\sum A_i \gamma_i + \Delta G_S = \textit{minimum}$$

- **Coherency Loss**

- **Glissil Interfaces** \longleftrightarrow **Solid/Liquid Interfaces**

- **Interface migration**

- **Interface controlled growth** \longleftrightarrow **Diffusion controlled growth**

**Q: What kind of interphase interfaces
in solid (α/β) exist?**

= coherent/ semi-coherent / incoherent/ complex semi-coherent

→ different interfacial free energy, γ

3.4 Interphase Interfaces in Solids

Interphase boundary

- different two phases : **different crystal structure**
different composition

coherent,
semicoherent
incoherent

3.4.1 Coherent interfaces

Disregarding chemical species, if the interfacial plane has the same atomic configuration in both phases,

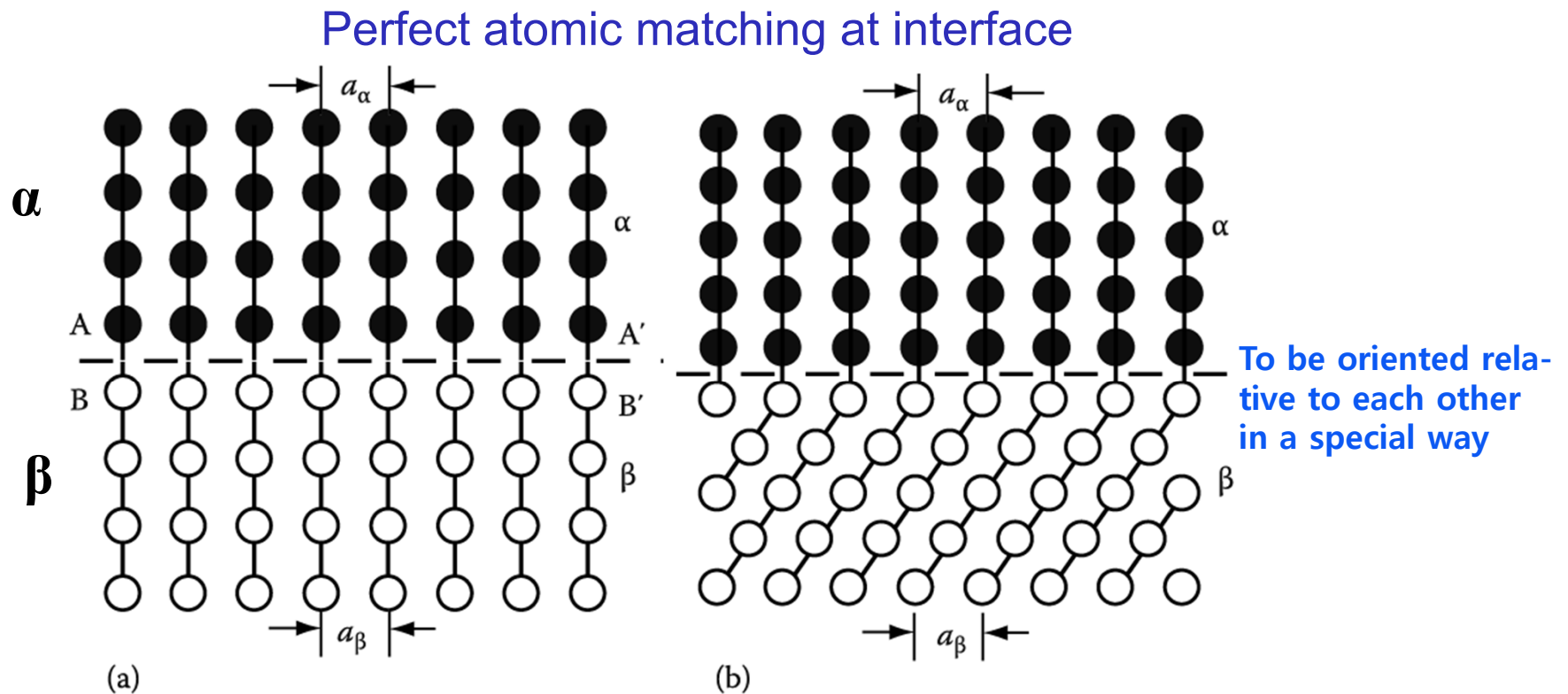


Fig. 3.32 Strain-free coherent interfaces. (a) Each crystal has a different chemical composition but the same crystal structure. (b) The two phases have different lattices

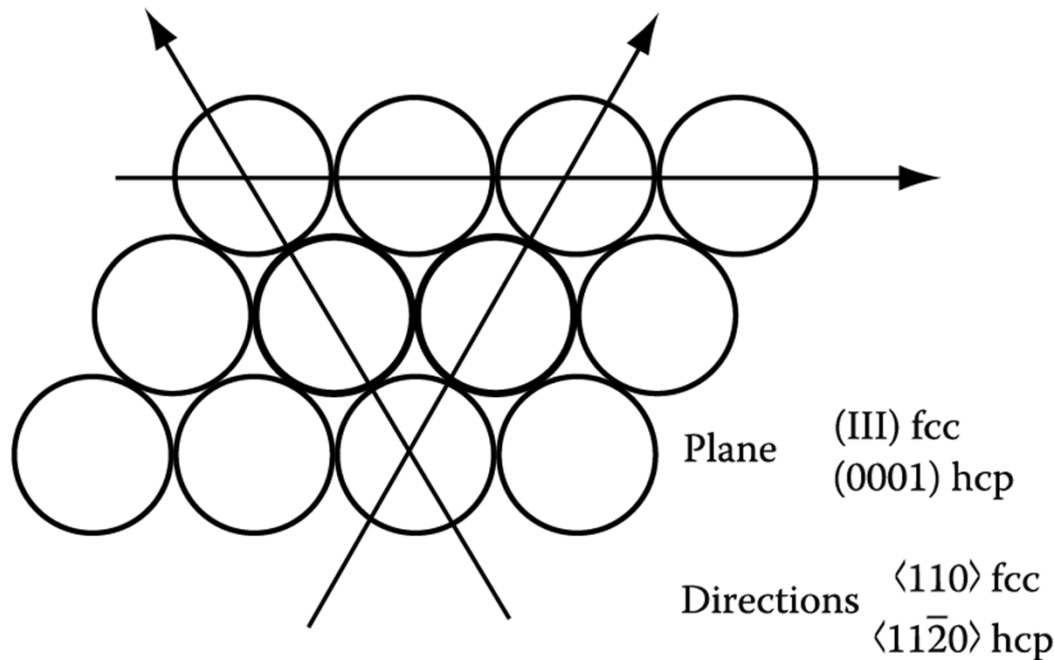
3.4.1 Coherent interfaces

Which plane and direction will be coherent between FCC and HCP?

: Interphase interface will make lowest energy and thereby the lowest nucleation barrier

ex) hcp silicon-rich κ phase in fcc copper-rich α matrix of Cu-Si alloy

→ the same atomic configuration
& interatomic distance



→ Orientation relation

$$\text{Cu } (111)_{\alpha} // (0001)_{\kappa} \text{ Si}$$

$$[\bar{1}10]_{\alpha} // [11\bar{2}0]_{\kappa}$$

$$\gamma_{\alpha-\kappa} \text{ of Cu-Si} \sim 1 \text{ mJm}^{-2}$$

In general,

$$\gamma (\text{coherent}) \sim 200 \text{ mJm}^{-2}$$

$$\begin{aligned} \gamma_{\text{coherent}} &= \gamma_{\text{structure}} + \gamma_{\text{chemical}} \\ &= \gamma_{\text{chemical}} \end{aligned}$$

$$\gamma (\text{coherent}) = \gamma_{\text{ch}} \quad 7$$

Fig. 3.33 The close-packed plane and directions in fcc and hcp structures.

hcp/ fcc interface: only one plane that can form a coherent interface

When the atomic spacing in the interface is not identical between the adjacent phase, what would happen?

Possible to maintain coherency by straining one or both crystal lattices.

→ lattice distortion

→ Coherency strain

→ strain energy

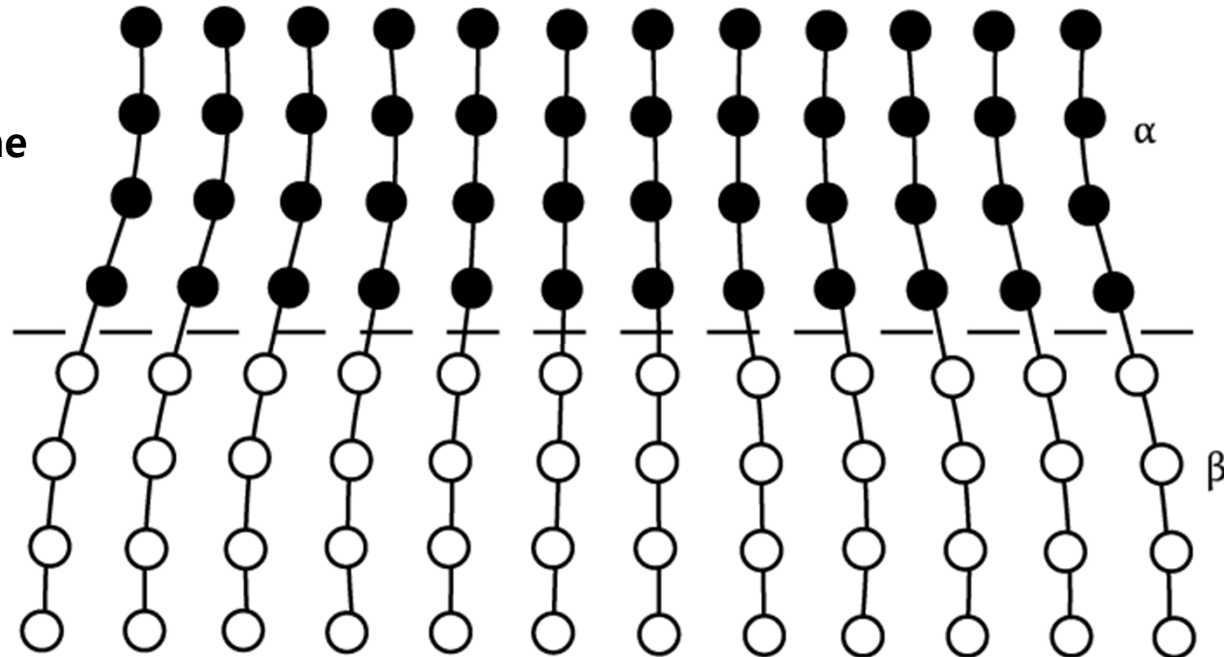
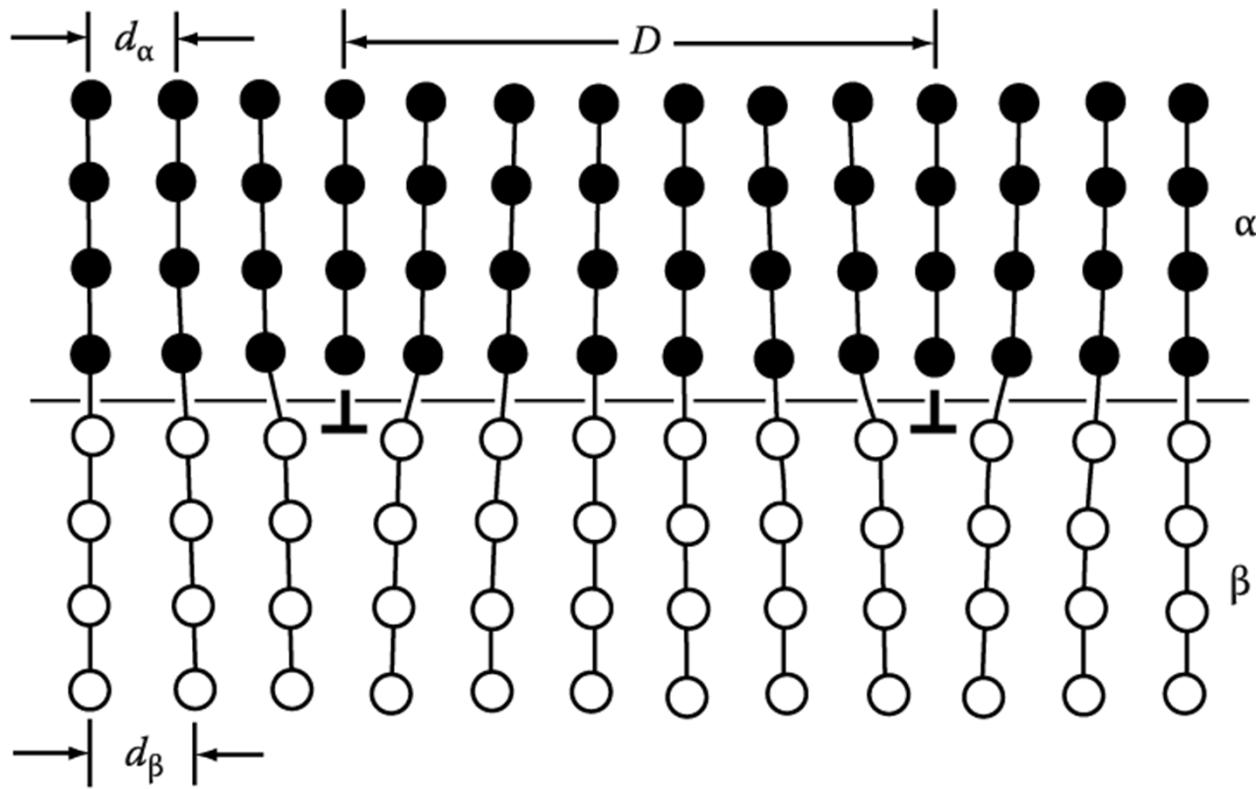


Fig. 3.34 A coherent interface with slight mismatch leads to coherency strains in the adjoining lattices.

The strains associated with a coherent interface raise the total energy of the system.

How can this coherent strain can be reduced?

If coherency strain energy is sufficiently large, → “misfit dislocations”
 → semi-coherent interface



Misfit between the two lattices

$$\delta = \frac{d_\beta - d_\alpha}{d_\alpha}$$

$\delta \sim$ small,

$$D = \frac{b}{\delta}$$

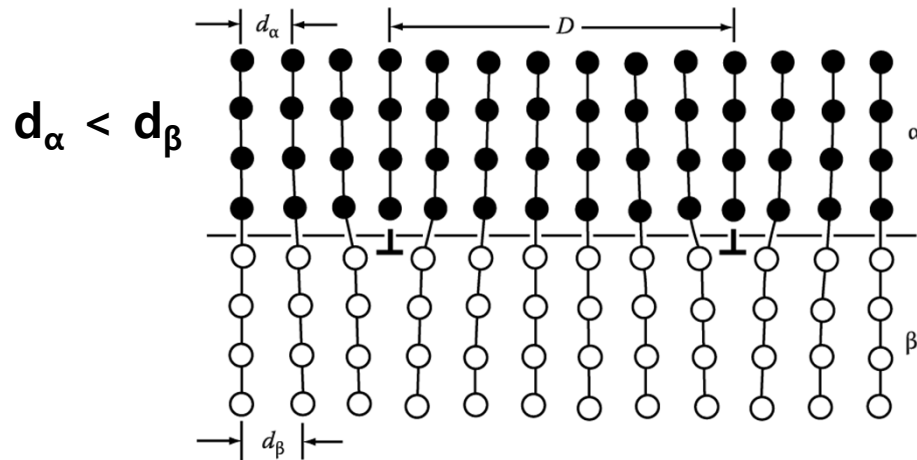
δ : misfit (disregistry)

b: Burgers vector of disl.

$$[b = (d_\alpha + d_\beta) / 2]$$

Fig. 3.35 A semi-coherent interface. The misfit parallel to the interface is accommodated by a series of edge dislocations.

(2) Semicoherent interfaces



$$\delta = (d_\beta - d_\alpha) / d_\alpha : \text{misfit}$$

→ D vs. δ vs. n

$$(n+1) d_\alpha = n d_\beta = D$$

$$\delta = (d_\beta / d_\alpha) - 1, (d_\beta / d_\alpha) = 1 + 1/n = 1 + \delta$$

→ $\delta = 1/n$

$$D = d_\beta / \delta \approx b / \delta \quad [b = (d_\alpha + d_\beta) / 2]$$

$\delta \sim$ small,

Burgers vector of dislocation

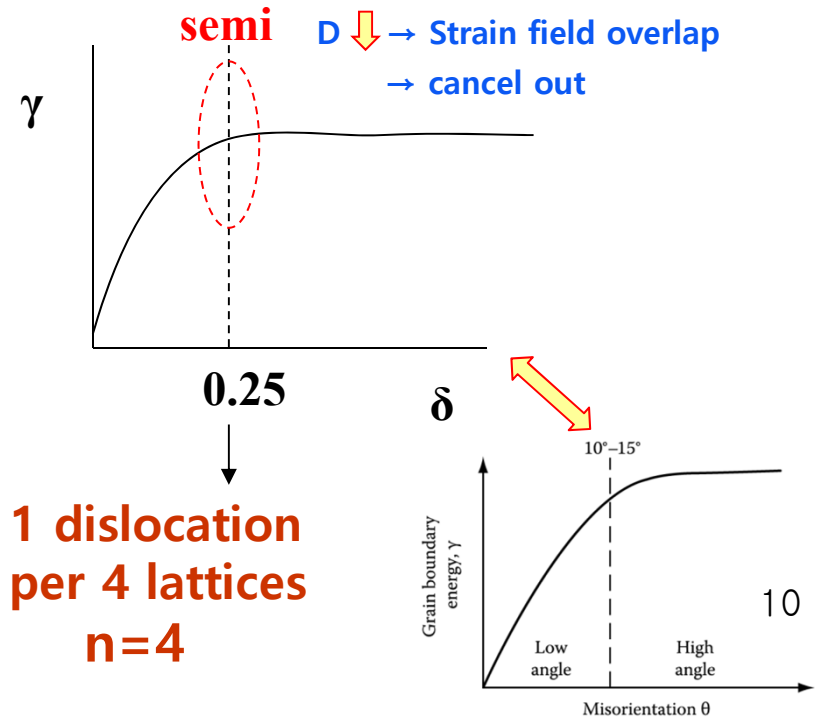
$$\gamma(\text{semicoherent}) = \gamma_{ch} + \gamma_{st}$$

γ_{st} → due to **structural distortions** caused by the misfit dislocations

$$\gamma_{st} \propto \delta \text{ for small } \delta$$

In general,

$\gamma(\text{semicoherent}) \sim 200 \sim 500 \text{ mJm}^{-2}$



3) Incoherent Interfaces ~ high angle grain boundary

1) $\delta > 0.25$ No possibility of good matching across the interface

2) different crystal structure (in general)

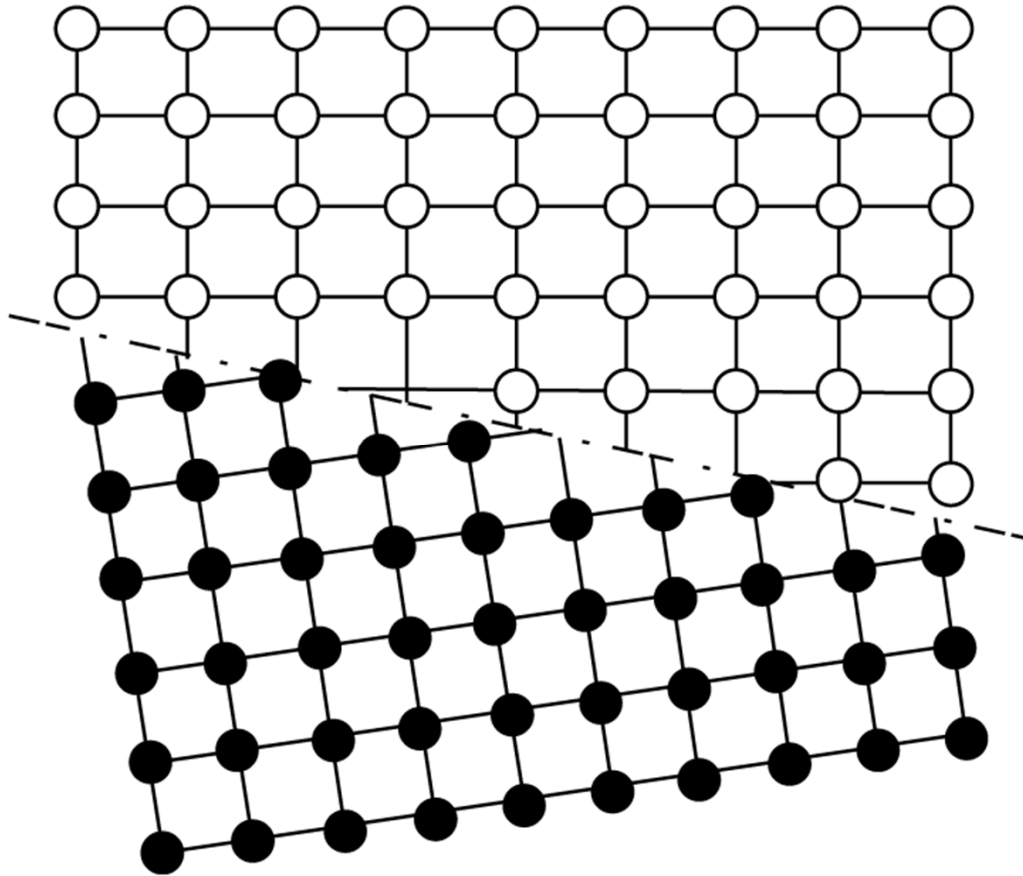
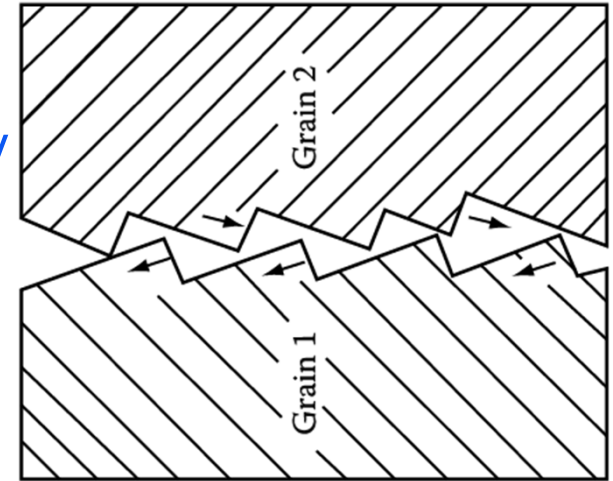


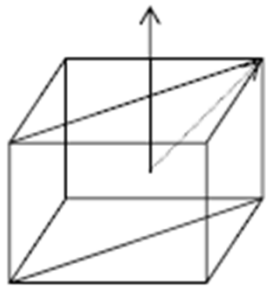
Fig. 3.37 An incoherent interface.



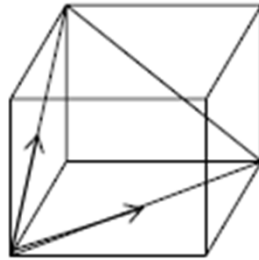
In general,
 γ (incoherent) $\sim 500\sim 1000 \text{ mJm}^{-2}$

incoherent

4) Complex Semicoherent Interfaces



$$a_{\alpha} = 2.87$$



$$a_{\gamma} = 3.57$$

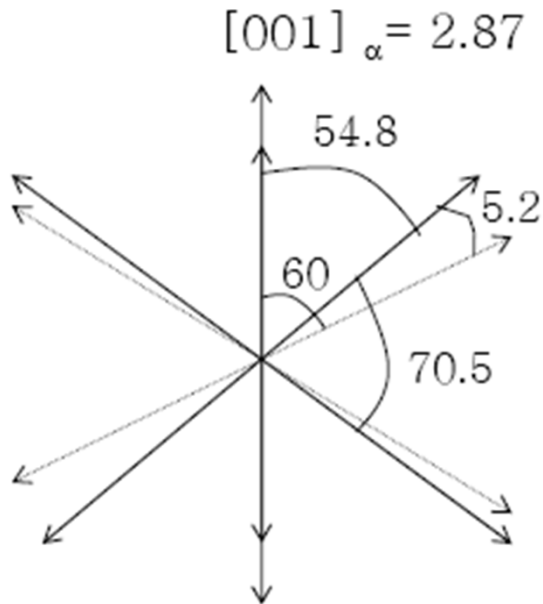
If **bcc** α is precipitated from **fcc** γ , which interface is expected?

Which orientation would make the lowest interface energy?

For fcc and bcc crystals ~ closest-pack planes in each phase almost parallel to each other

Nishiyama-Wasserman (N-W) Relationship

$$(110)_{bcc} // (111)_{fcc}, \quad [001]_{bcc} // [\bar{1}01]_{fcc}$$



Kurdjumov-Sachs (K-S) Relationships

$$(110)_{bcc} // (111)_{fcc}, \quad [1\bar{1}1]_{bcc} // [0\bar{1}1]_{fcc}$$

(The only difference between these two is a rotation in the closest-packed planes of 5.26°.)

Complex Semicoherent Interfaces

Semicoherent interface observed at boundaries formed by low-index planes.
(atom pattern and spacing are almost equal.)

N-W relationship

Good fit is restricted to small diamond-shaped areas that only contain ~8% of the orientation relationship.

A similar situation can be shown to exist for the K-S orientation relationship.

⇒ **But,**
impossible to form a large interfaces
→ Incoherent interface

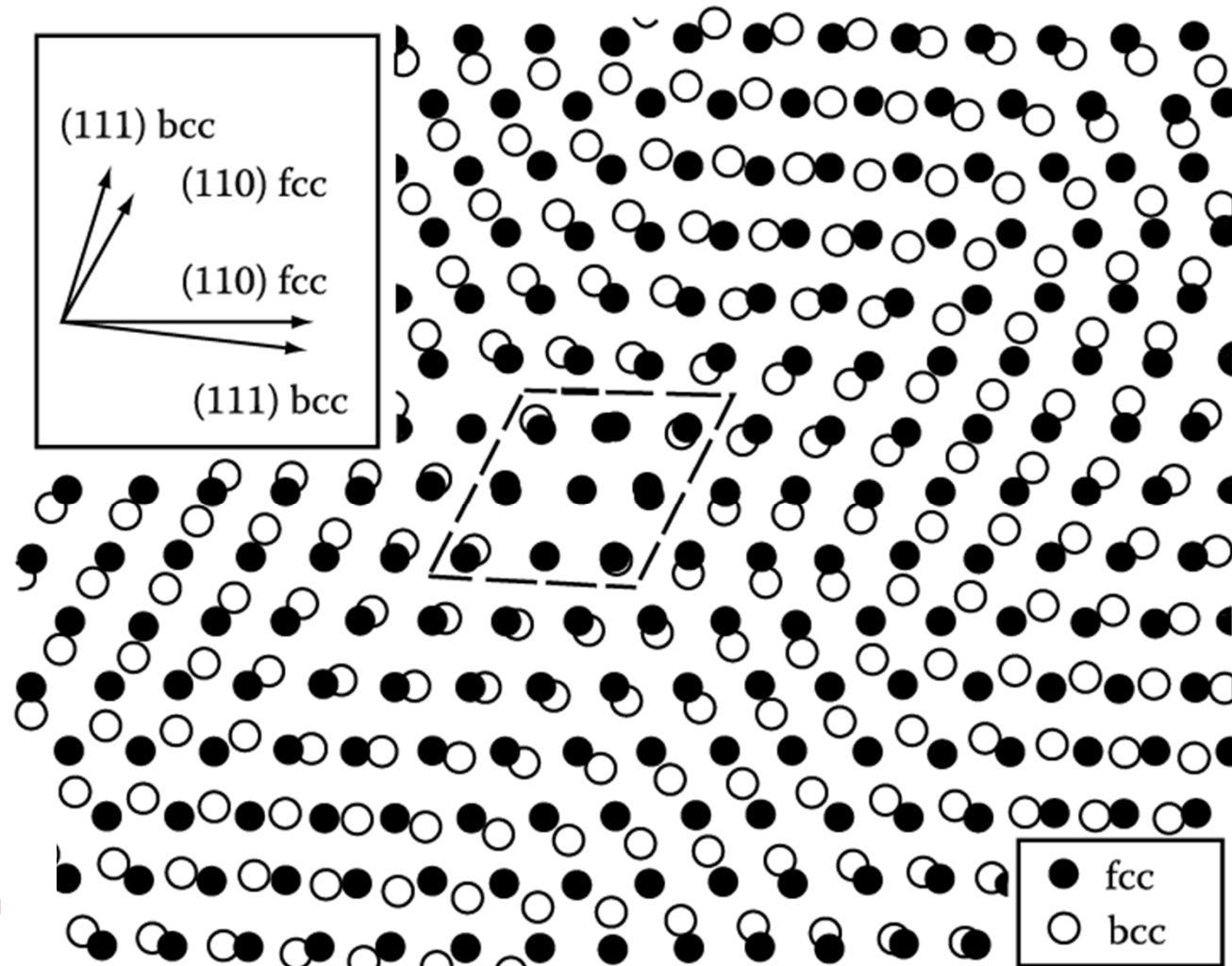
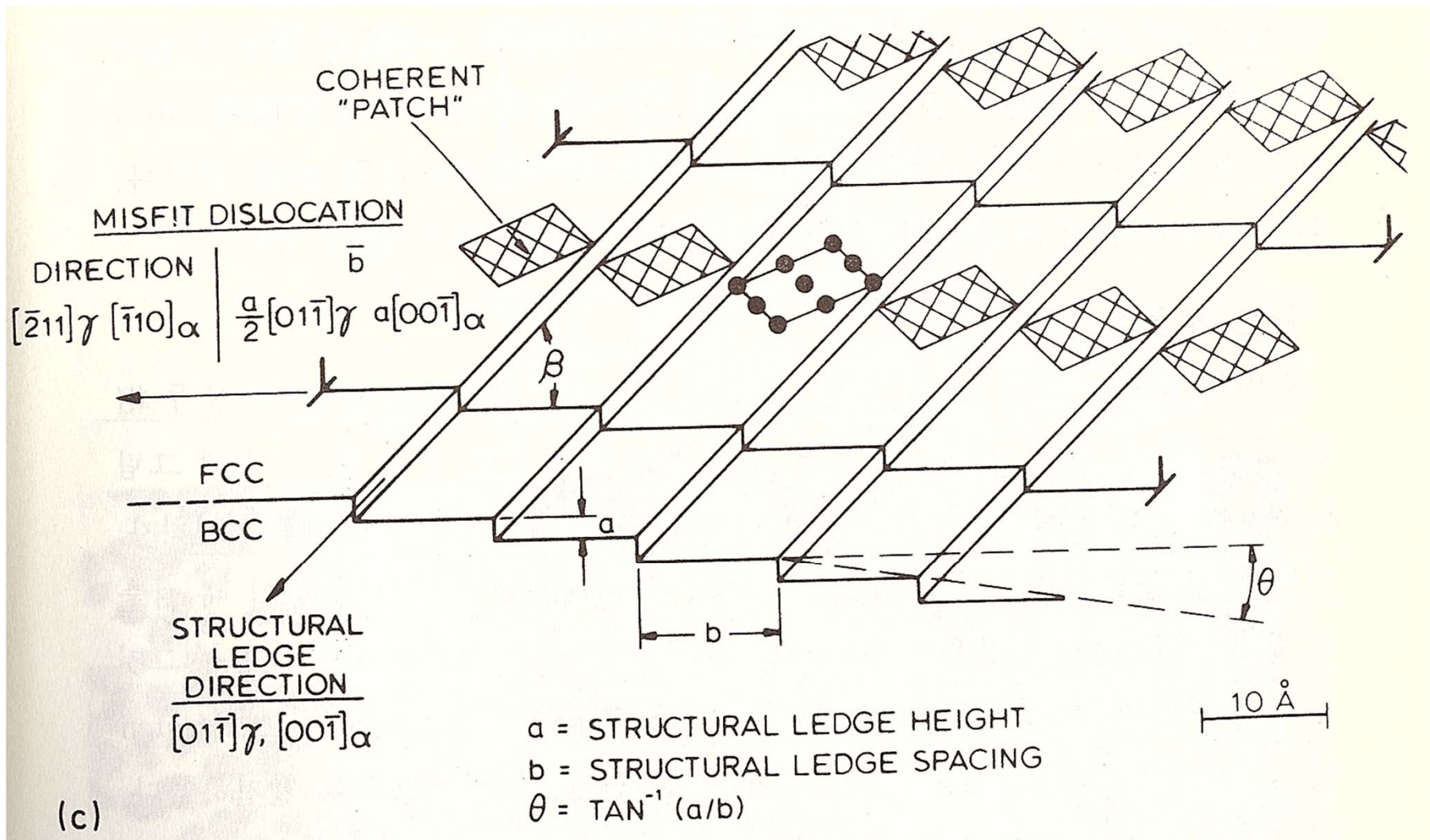


Fig. 3.38 Atomic matching across a (111)fcc/(110)bcc interface bearing the NW orientation relationship for lattice parameters closely corresponding to the case of fcc and bcc iron.

Complex Semicoherent Interfaces



The degree of coherency can, however, be greatly increased if a macroscopically irrational interface is formed. **The detailed structure of such interfaces is, however, uncertain** due to their complex nature.

3.4 Interphase Interfaces in Solids

Interphase boundary - different two phases : **different crystal structure**
different composition

coherent,

Perfect atomic matching at interface

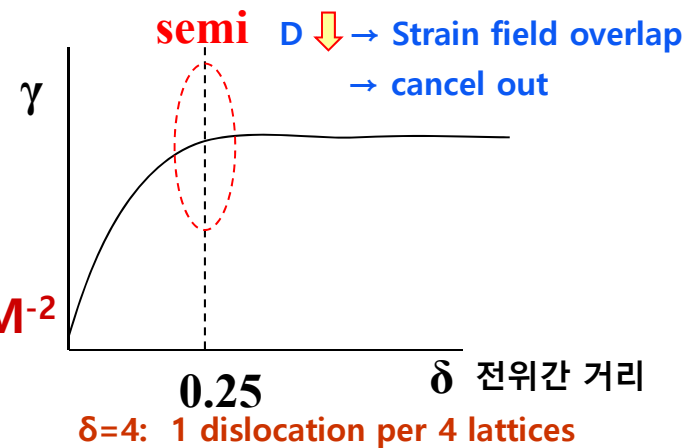
γ (coherent) = γ_{ch} γ (coherent) \sim 200 mJM⁻²

semicoherent

γ (semicoherent) = $\gamma_{ch} + \gamma_{st}$

γ_{st} → due to structural distortions caused by the misfit dislocations

γ (semicoherent) \sim 200~500 mJM⁻²



incoherent

1) $\delta > 0.25$ No possibility of good matching across the interface

2) different crystal structure (in general)

γ (incoherent) \sim 500~1000 mJM⁻²

Complex Semicoherent Interfaces

Nishiyama-Wasserman (N-W) Relationship

Kurdjumov-Sachs (K-S) Relationships

(The only difference between these two is a rotation in the closest-packed planes of 5.26°.)

The degree of coherency can, however, be greatly increased if a macroscopically irrational interface is formed.

Q: How is the second-phase shape determined?

If misfit is small,
Equilibrium shape of a coherent
precipitate or zone **can only**
be predicted from the "γ-plot"

$$\sum A_i \gamma_i$$

⇒
Misfit

$$\sum A_i \gamma_i + \Delta G_S = \textit{minimum}$$

"γ-plot" + "Elastic strain energy"

Lowest total interfacial free energy
by optimizing the shape of the precipitate and its orientation relationship

Fully coherent precipitates

γ_{ch}

different composition

⇒

$\gamma_{ch} + \textit{Lattice misfit}$

Coherency strain energy

⇒

Incoherent inclusions

$\gamma_{ch} + \textit{Volume Misfit } \Delta = \frac{\Delta V}{V}$

Chemical and structural interfacial E

(a) Precipitate shapes : $\sum A_i \gamma_i$ ↓

(b) Calculation of misfit strain energy

3.4.2 Second-Phase Shape: Interfacial Energy Effects

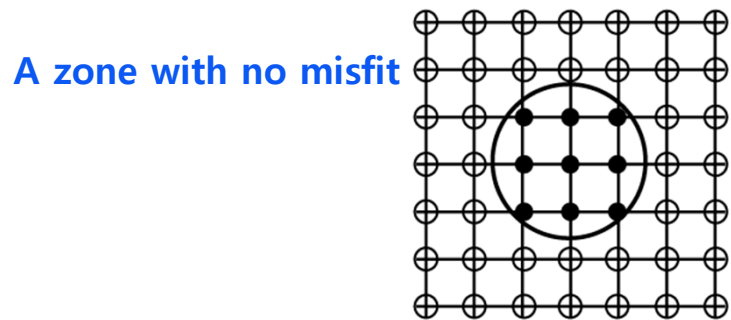
How is the second-phase shape determined? $\sum A_i \gamma_i = \text{minimum}$

Lowest total interfacial free energy

by optimizing the shape of the precipitate and its orientation relationship

A. Fully Coherent Precipitates (G.P. Zone)

- If α , β have the same structure & a similar lattice parameter
- Happens during early stage of many precipitation hardening
- Good match \Rightarrow can have any shape \Rightarrow **spherical**

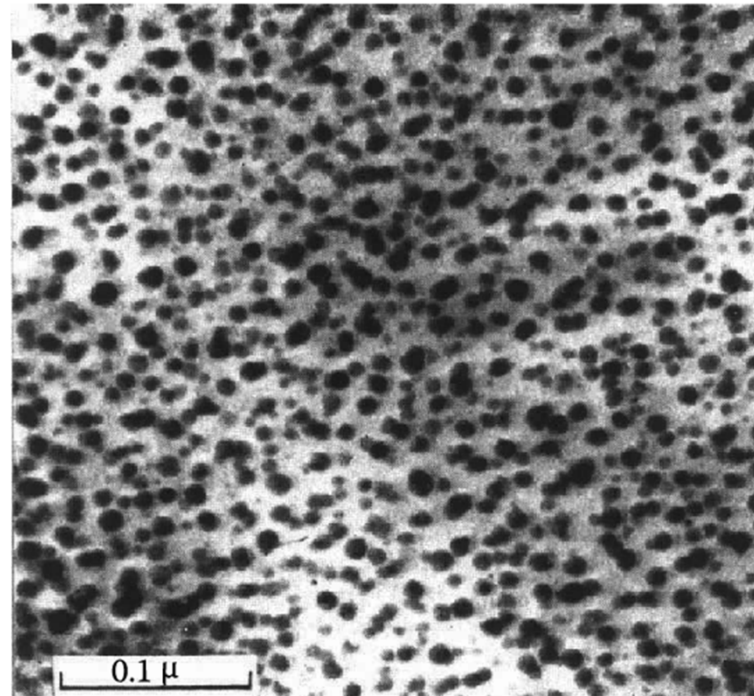


(a)

GP(Guinier- Preston) Zone
in Al – Ag Alloys

$$\varepsilon_a = \frac{r_A - r_B}{r_A} = 0.7\%$$

\rightarrow negligible contribution
to the total free energy



(b) Ag-rich GP zones (Dia. \sim 10 nm) in Al-4at% Ag alloy

B. Partially Coherent Precipitates

- α , β have different structure and one plane which provide close match
- Coherent or Semi-coherent in one Plane;
Disc Shape (also plate, lath, needle-like shapes are possible)

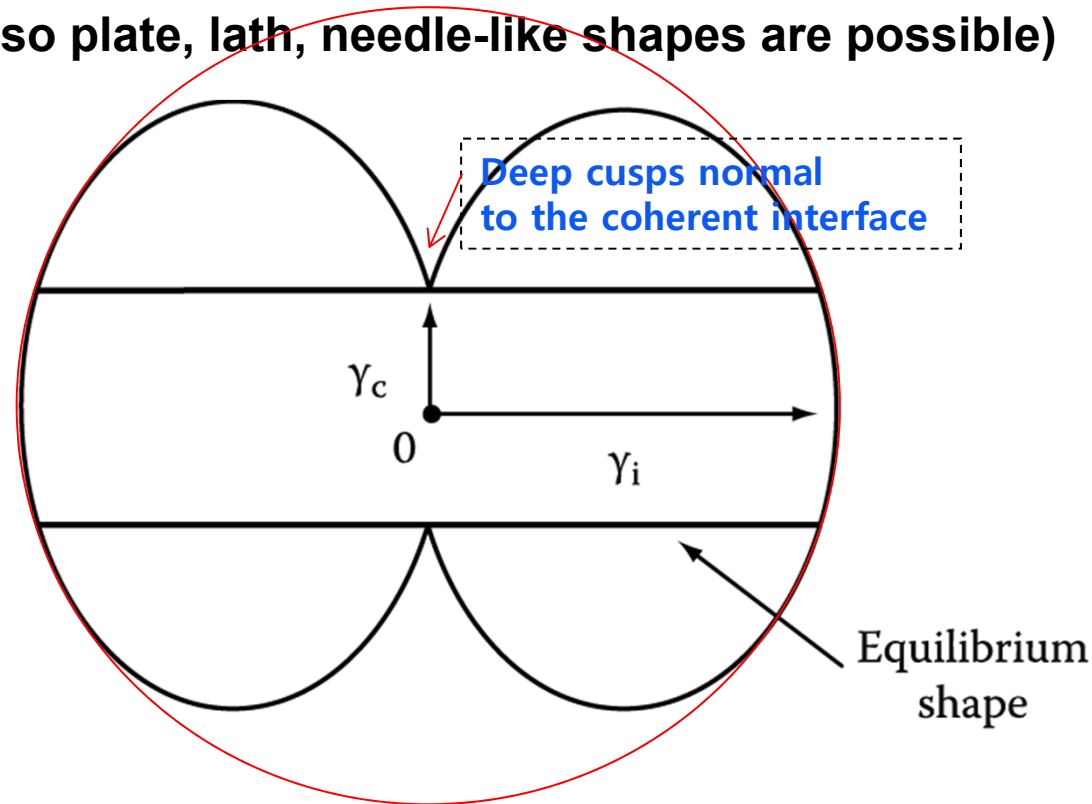


Fig. 3.40 A section through a γ -plot for a precipitate showing one coherent or semi-coherent interface, together with the equilibrium shape (a disc).

Precipitate shapes observed in practice

- ~ not equilibrium shape through a γ -plot why?
- 1) misfit strain E effects ~ ignored.
 - 2) different growth rates depending on directions

hcp γ' Precipitates in Al – 4% Ag Alloys \rightarrow plate

Semicoherent broad face parallel to the $\{111\}_\alpha$ matrix planes
(usual hcp/fcc orientation relationship)

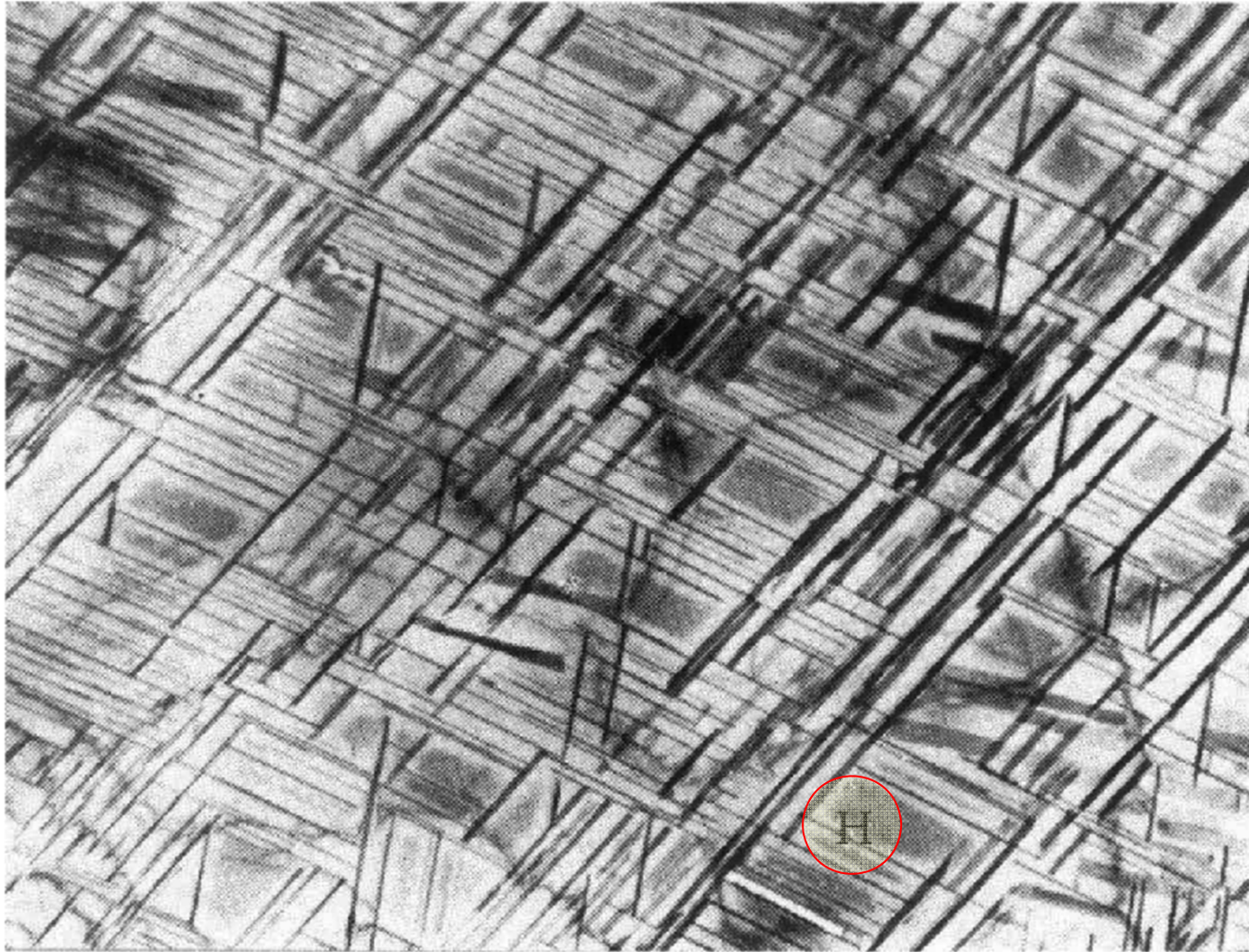
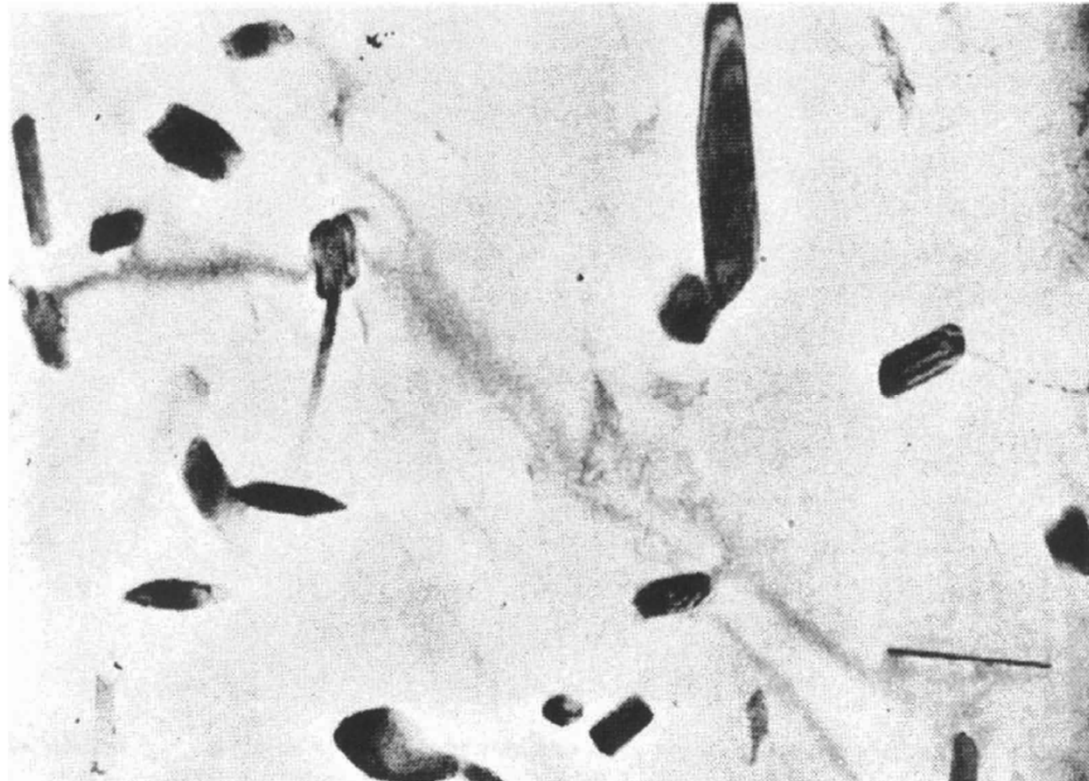
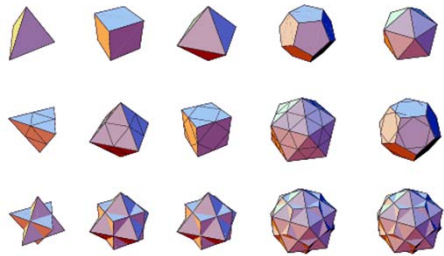


Fig. 3. 42 Electron micrograph showing the Widmanstatten morphology of γ' precipitates in an Al-4 atomic % Ag alloy. GP zones can be seen between the γ' e.g. at H (x 7000).

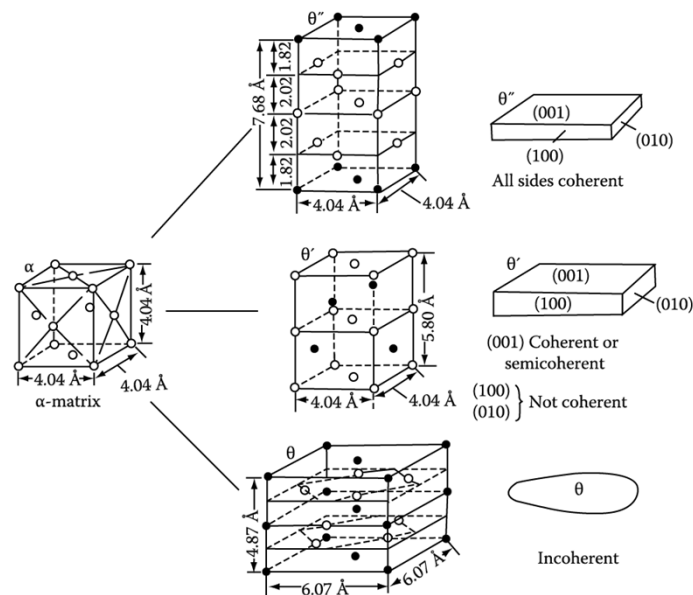
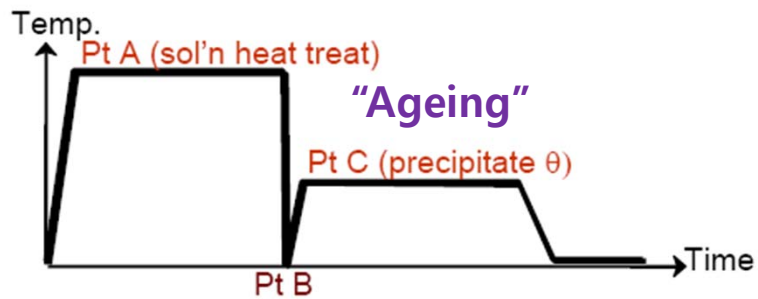
C. Incoherent precipitates

- when α , β have completely different structure \Rightarrow Incoherent interfaces
or When the two lattices are in a random orientation
- Interface energy is high for all plane \Rightarrow spherical shape
with smoothly curved interface
- Polyhedral shapes: certain crystallographic planes of the inclusion lie at cusps in the γ -plot



θ phase in Al - Cu alloys (Al_2Cu)

Q: Example of Second-Phase Shape precipitates from solid solution in Al-Cu alloys



G.P. Zone



θ'' , all coherent



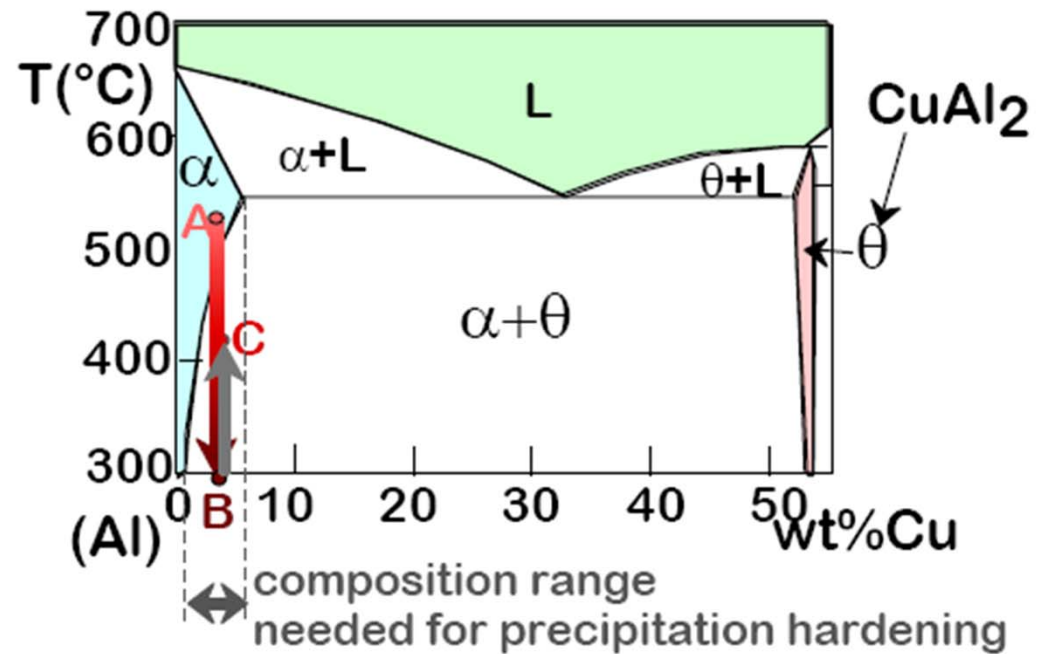
θ' , partially coherent



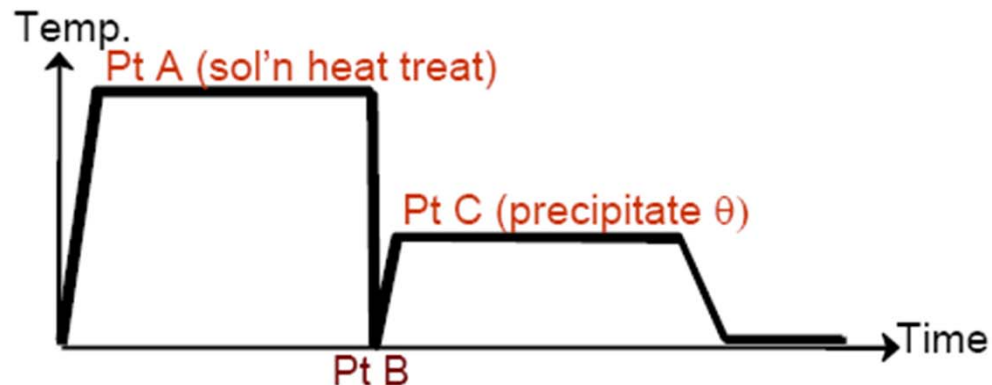
θ , incoherent

Precipitation Hardening

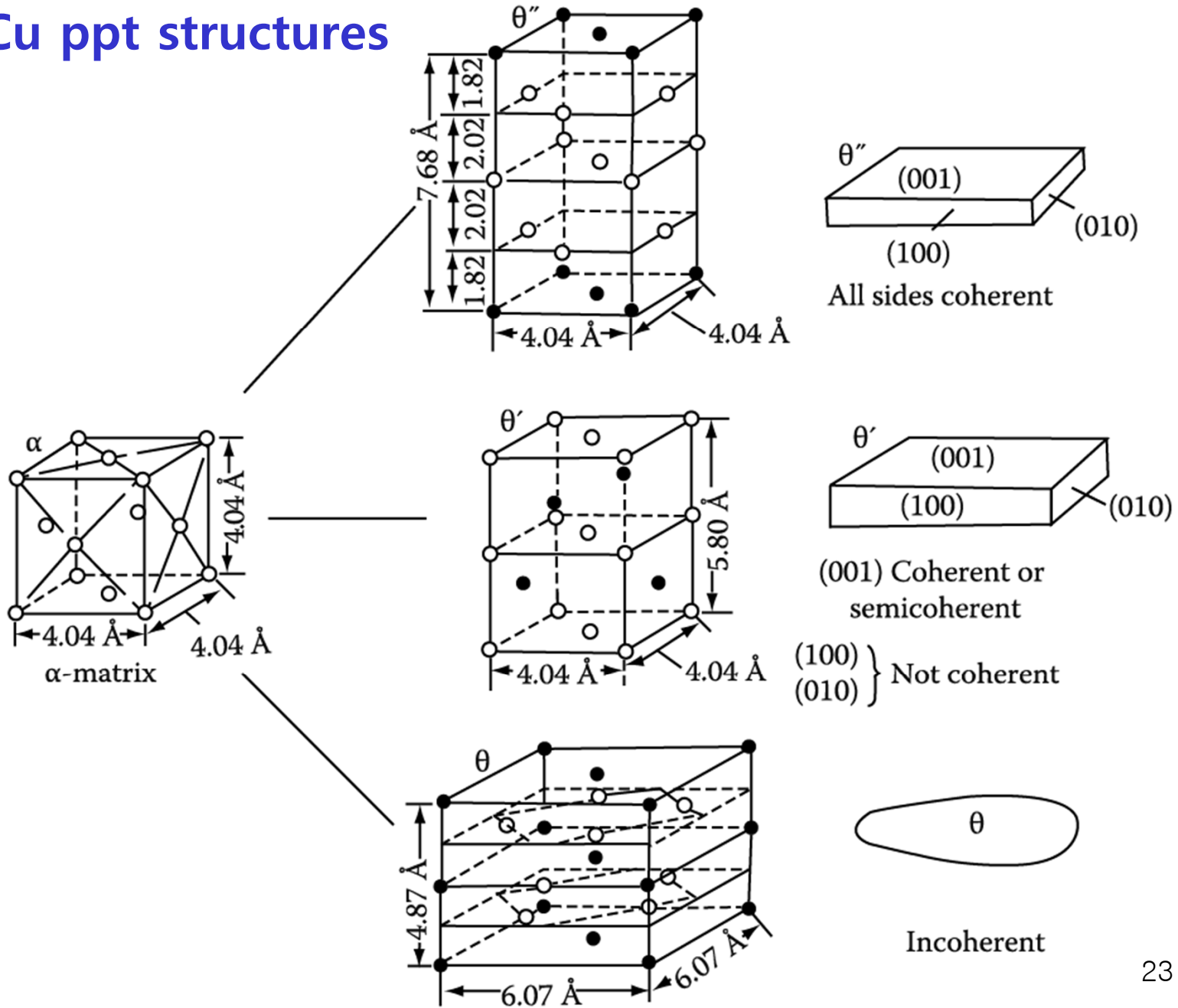
- Ex: Al-Cu system
- Procedure:
 - *Pt A*: solution heat treat (get a solid solution)
 - *Pt B*: quench to room temp.
 - *Pt C*: reheat to nucleate small θ crystals within α crystals.



$\alpha + \theta \rightarrow$ Heat ($\sim 550^{\circ}\text{C}$) \rightarrow Quench (0°C) $\rightarrow \alpha$ (ssss) \rightarrow Heat/age ($\sim 150^{\circ}\text{C}$) $\alpha + \theta_{\text{ppt}}$

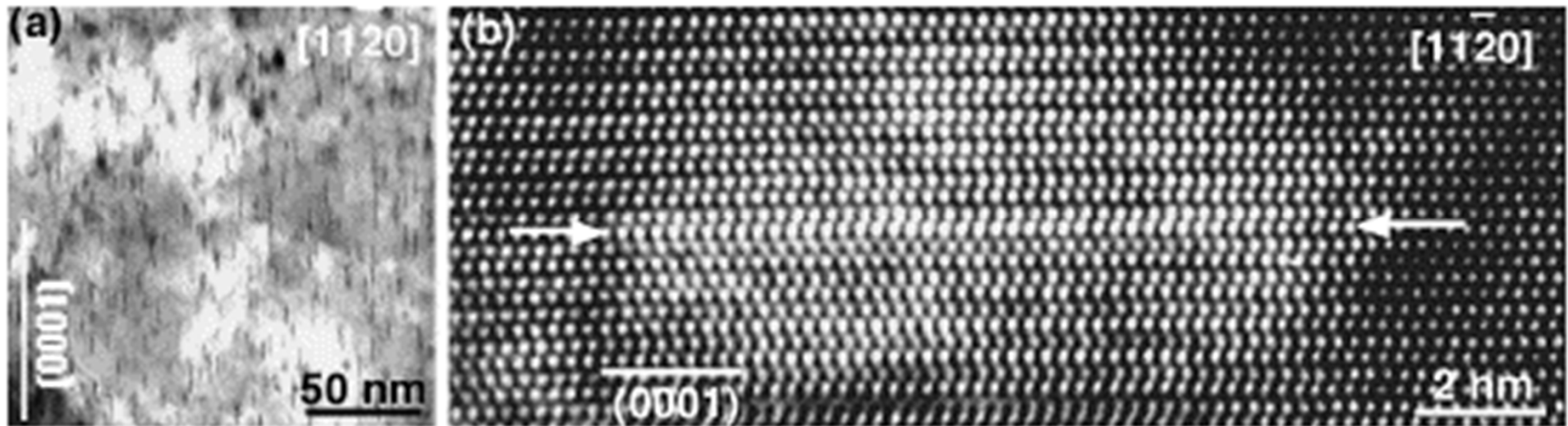
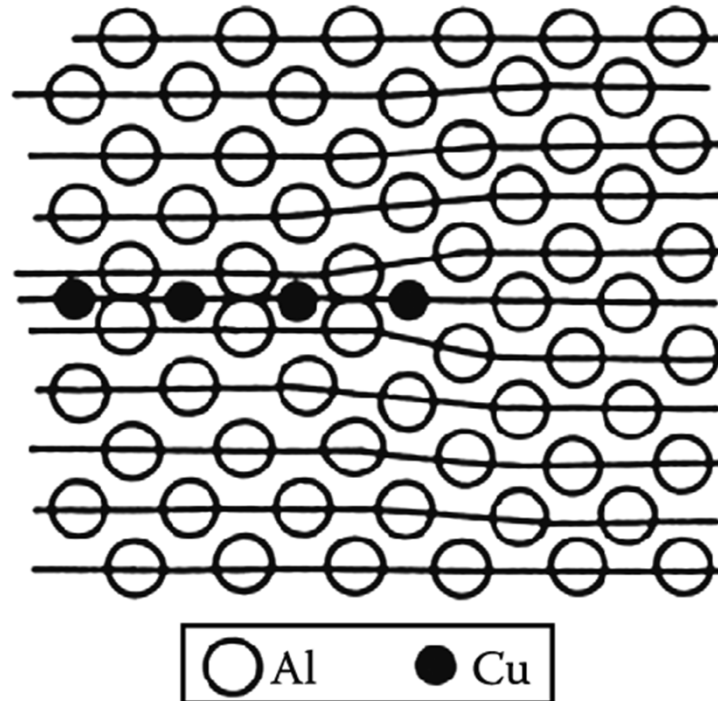


Al-Cu ppt structures



Al-Cu ppt structures

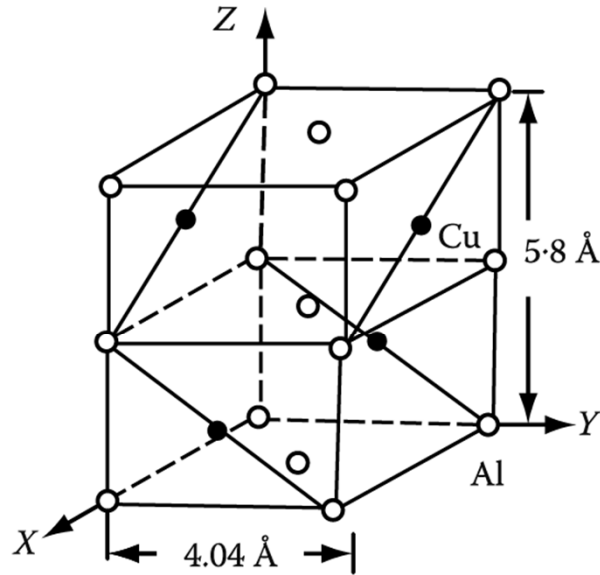
GP zone structure



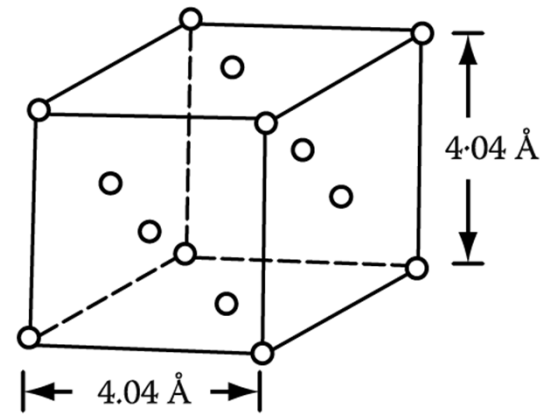
(a) Bright-field TEM image showing G.P. zones, and (b) HRTEM image of a G.P. zone formed on a single $(0\ 0\ 0\ 1)_\alpha$ plane. Electron beam is parallel to $[11\bar{2}0]$ in both (a) and (b).

θ' Phase Al-Cu Alloys

Semicoherent broad face parallel to the $\{100\}_\alpha$ matrix planes (habit plane)



(a) The unit cell of the θ' precipitate in Al-Cu alloys



(b) The unit cell of the matrix

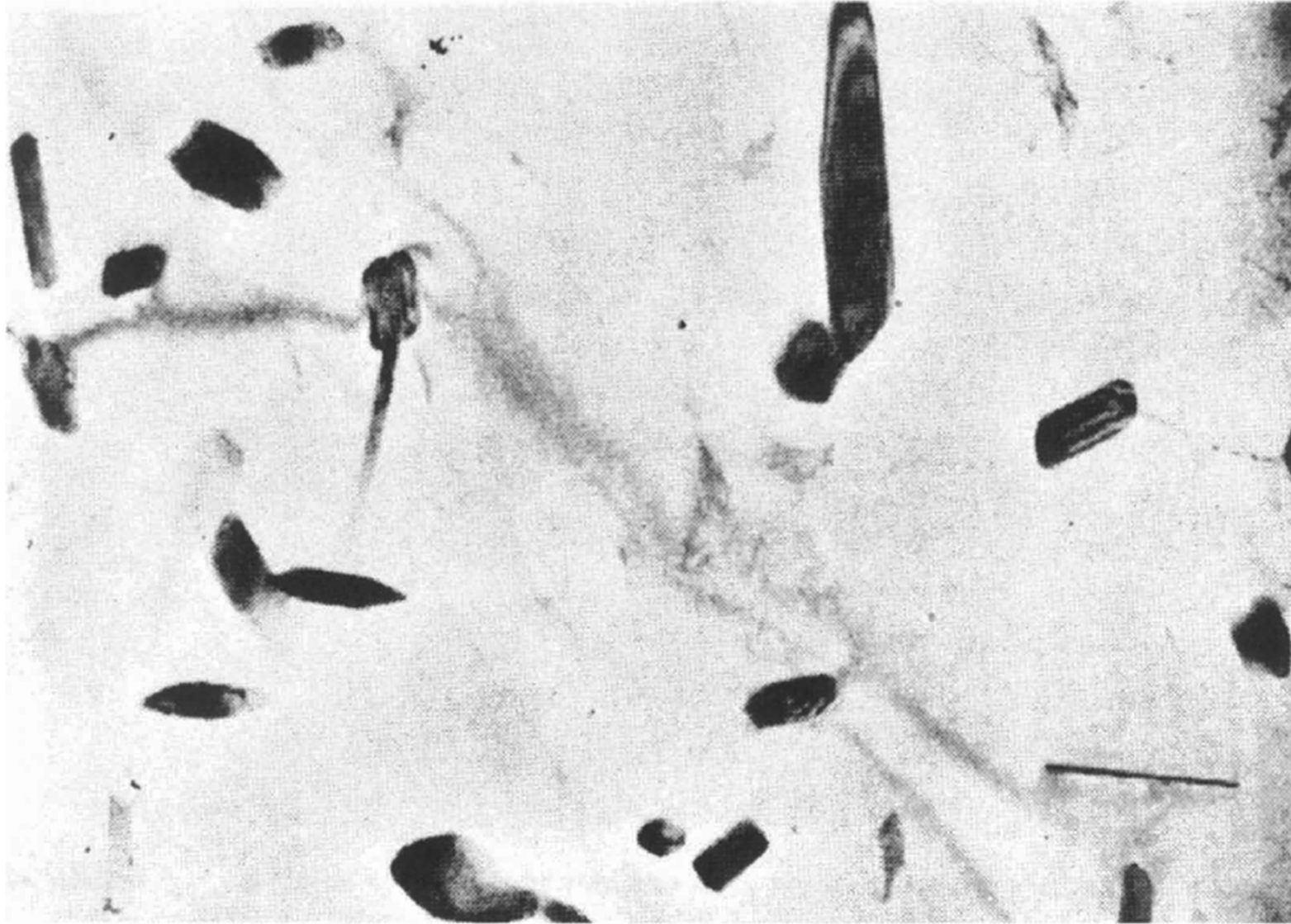
Orientation relationship between α and θ'

$$(001)_{\theta'} // (001)_{\alpha} \quad [100]_{\theta'} // [100]_{\alpha}$$

→ Cubic symmetry of the Al-rich matrix (α) ~ many possible orientations for the precipitate plates within any given grain

$\left. \begin{array}{l} \text{S phase in Al-Cu-Mg alloys ; Lath shape} \\ \beta' \text{ phase in Al-Mg-Si alloys ; Needle shape} \end{array} \right\} \text{Widmanstätten morphology}$

θ phase in Al – Cu alloys (Al_2Cu)



- **Polyhedral shapes:** certain crystallographic planes of the inclusion lie at cusps in the γ -plot

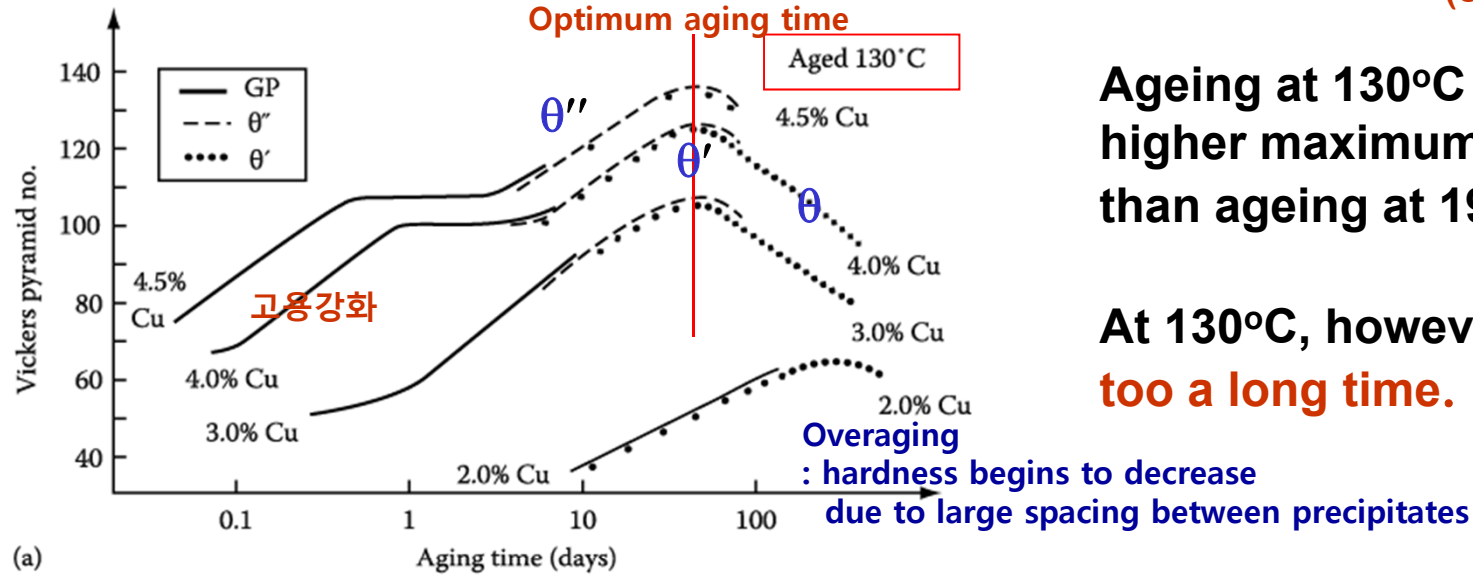
5.5.4. Age Hardening

Transition phase precipitation → great improvement in the mechanical properties

Coherent precipitates → highly strained matrix → dislocations~forced during deformation

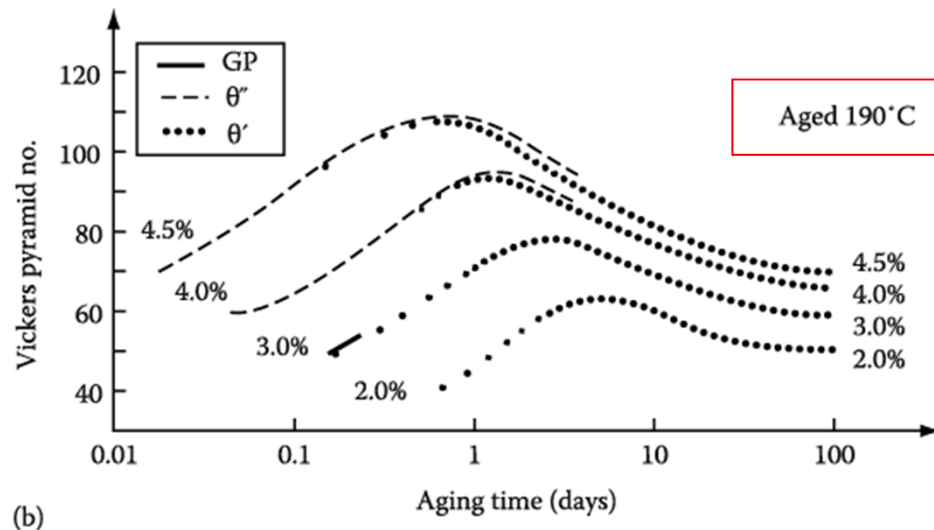
Hardness vs. Time by Ageing

Maximum hardness~ largest fraction of θ''
(coherent precipitates)



Ageing at 130°C produces higher maximum hardness than ageing at 190°C.

At 130°C, however, it takes **too a long time.**



How can you get the high hardness for the relatively short ageing time?

Double ageing treatment
first below the GP zone solvus
→ fine dispersion of GP zones
then ageing at higher T.

Finer precipitate distribution

Fig. 5. 37 Hardness vs. time for various Al-Cu alloys at (a) 130 °C (b) 190 °C

Precipitates on Grain Boundaries

Formation of a second-phase particle at the interfaces with two differently oriented grains

- 1) incoherent interfaces with both grains
- 2) a coherent or semi-coherent interface with one grain and an incoherent interface with the other,
- 3) coherent or semi-coherent interface with both grains

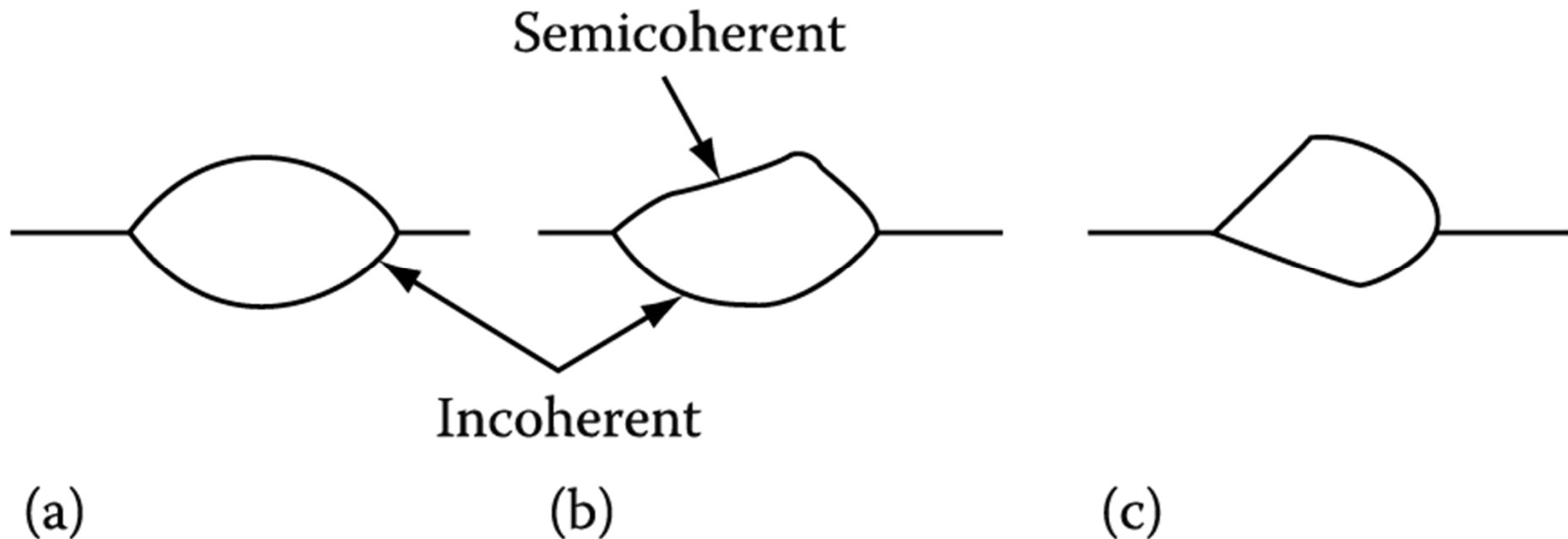


Fig. 3. 45 Possible morphologies for grain boundary precipitates. Incoherent interfaces smoothly curved. Coherent or semicoherent interface planar.

Precipitates on Grain Boundaries

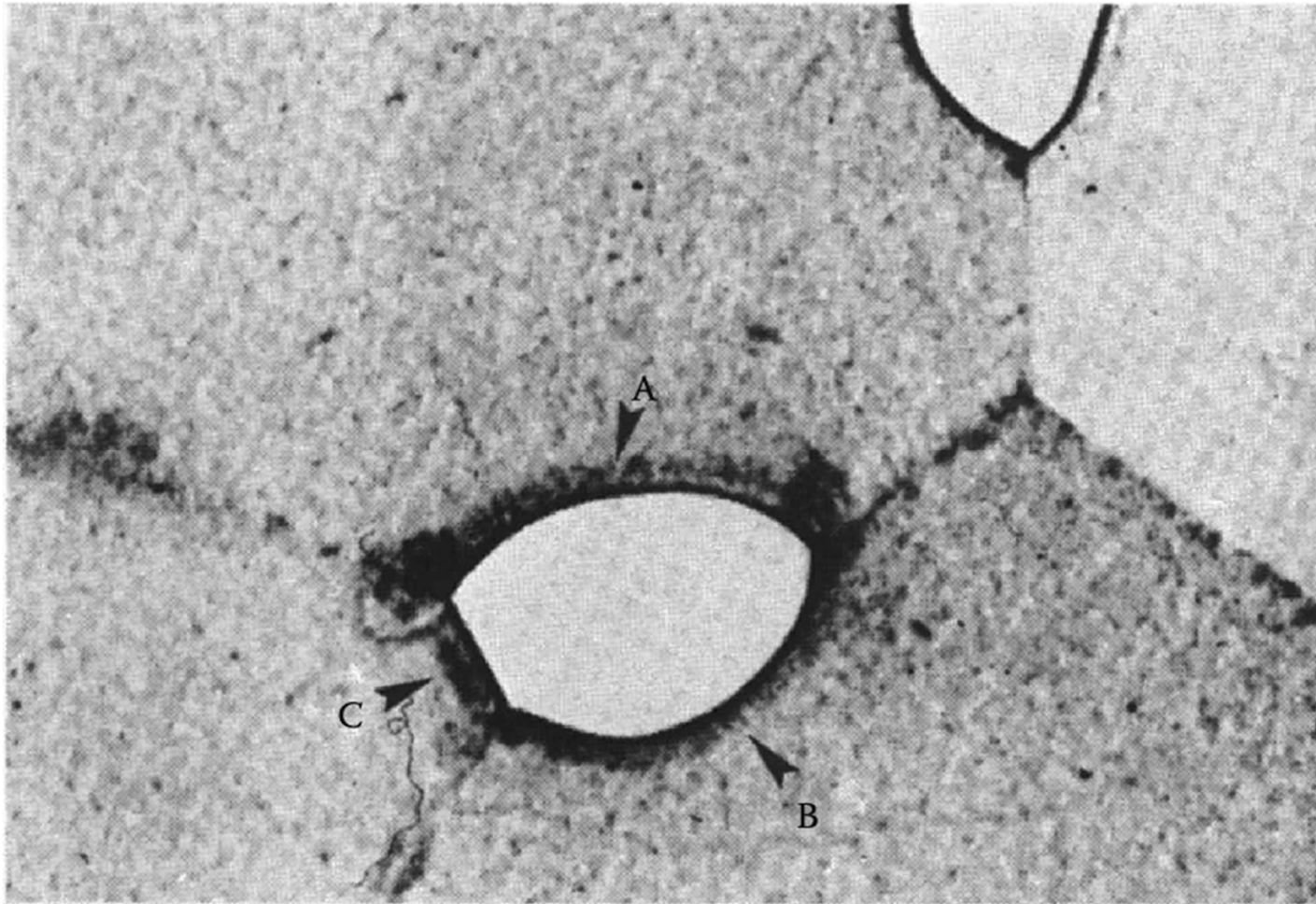
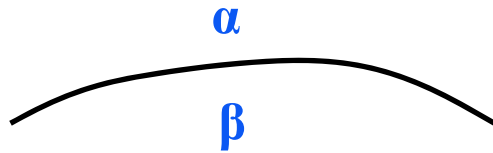


Fig. 3. 46 An α precipitate at a grain boundary triple point in an $\alpha - \beta$ Cu-In alloy. Interfaces A and B are incoherent while C is semicoherent (x 310).

A, B; Incoherent, C; Semi-coherent or coherent

3.4 Interphase Interfaces in Solids (α/β) $\sum A_i \gamma_i + \Delta G_S = \text{minimum}$

1) Interphase boundary - different two phases : different crystal structure
different composition



Coherent/ Semicoherent/ Incoherent
Complex Semicoherent

Fully coherent precipitates

γ_{ch}
different composition

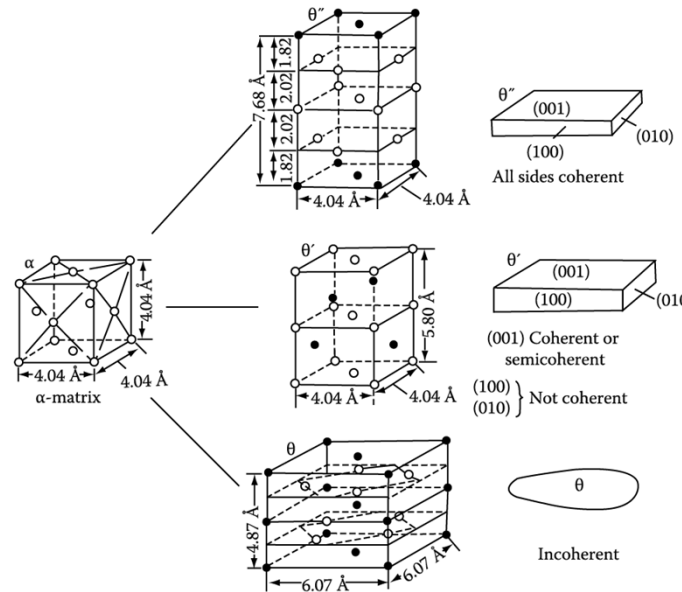
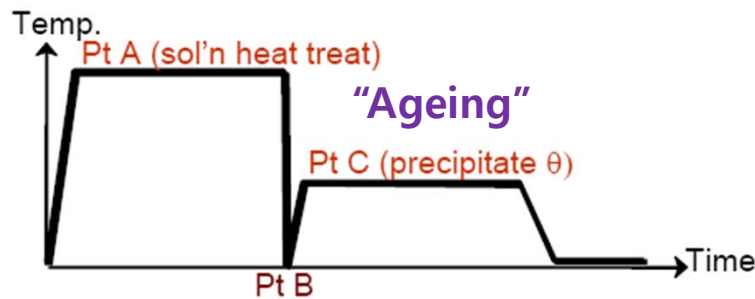


$\gamma_{ch} + \text{Lattice misfit}$
Coherency strain energy



Incoherent inclusions
 $\gamma_{ch} + \text{Volume Misfit } \Delta = \frac{\Delta V}{V}$
Chemical and structural interfacial E

2) Second-Phase Shape: precipitate from solid solution in Al-Cu alloys



G.P. Zone



θ'' , all coherent



θ' , partially coherent



θ , incoherent

Q: How is the second-phase shape determined?

$$\sum A_i \gamma_i + \Delta G_S = \text{minimum}$$

γ - plot + misfit strain E

Lowest total interfacial free energy

by optimizing the shape of the precipitate and its orientation relationship

Fully coherent precipitates

γ_{ch}

different composition



$\gamma_{ch} +$ *Lattice misfit*

Coherency strain energy



Incoherent inclusions

$\gamma_{ch} +$

$$\text{Volume Misfit } \Delta = \frac{\Delta V}{V}$$

Chemical and structural interfacial E

(a) Precipitate shapes

(b) Calculation of misfit strain energy

3.4.3. Second-Phase Shape: Misfit Strain Effects

If misfit is small,
Equilibrium shape of a coherent precipitate or zone **can only be predicted from the "γ-plot"**

$$\sum A_i \gamma_i$$

⇒
Misfit

$$\sum A_i \gamma_i + \Delta G_S = \text{minimum}$$

"γ-plot" + "Elastic strain energy"

A. Fully Coherent Precipitates

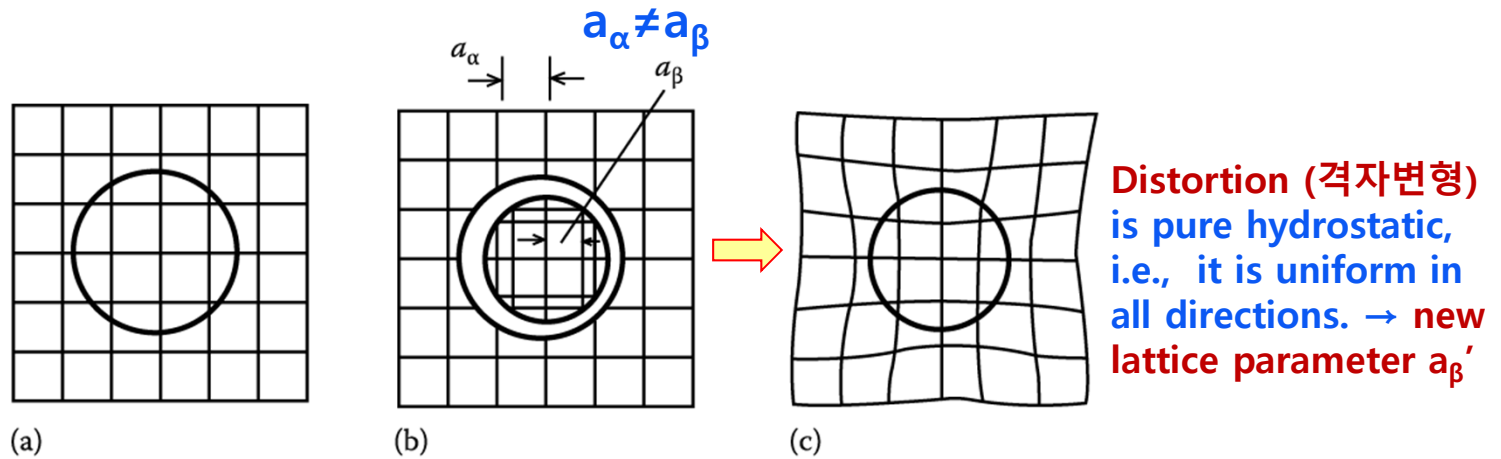


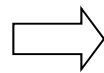
Fig. 3. 47 The origin of coherency strains. The number of lattice points in the hole is conserved.

Unconstrained Misfit

Constrained Misfit

구속되지 않은
불일치도

$$\delta = \frac{a_\beta - a_\alpha}{a_\alpha}$$



구속된
불일치도

$$\varepsilon = \frac{a'_\beta - a_\alpha}{a_\alpha}$$

① If $E_\beta = E_\alpha, \nu = 1/3 \rightarrow \varepsilon = \frac{2}{3} \delta$
Poisson's ratio

②

In practice, different elastic constants $E_\beta \neq E_\alpha \rightarrow 0.5\delta \leq \varepsilon \leq \delta$

if thin disc-type precipitate,

→ In situ misfit is no longer equal in all directions

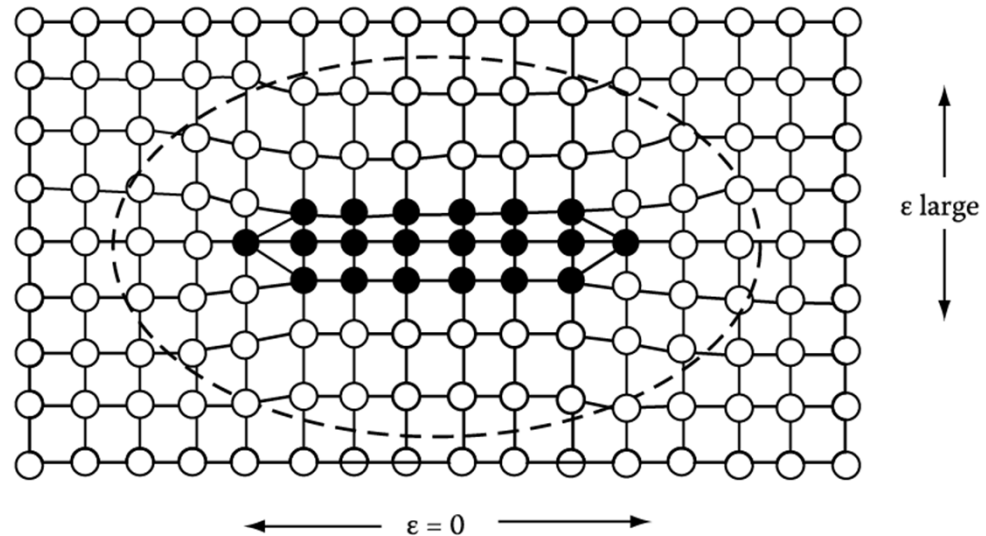


Fig. 3. 48 For a coherent thin disc there is **little misfit parallel to the plane of the disc.** **Maximum misfit is perpendicular to the disc.** → reduction in coherency strain E

* Total elastic energy (ΔG_s) depends on the "shape" and "elastic properties" of both matrix and inclusion.

Elastically Isotropic Materials
& $E_\beta = E_\alpha$

$\Delta G_s \rightarrow$ independent of the shape of the precipitate

$$\Delta G_s = 4\mu\delta^2 \cdot V \quad (\text{If } \nu=1/3)$$

here, μ = shear modulus of the matrix,

V = volume of the unconstrained hole in the matrix

Elastically Anisotropic Materials & $E_\beta \neq E_\alpha$

$\Delta G_s \rightarrow$ dependent of the shape of the precipitate

ΔG_s^{\min} : if inclusion is hard \rightarrow sphere/ soft \rightarrow disc shape

Atom radius (\AA) Al : 1.43 Ag : 1.44 Zn : 1.38 Cu : 1.28

Zone Misfit (δ) - + 0.7% - 3.5% - 10.5%

GP Zone Shape

Equilibrium shape

sphere sphere

disc

$$\sum A_i \gamma_i + \Delta G_s = \text{minimum}$$

Interfacial E effect dominant

$\delta < 5\%$

strain E effect dominant

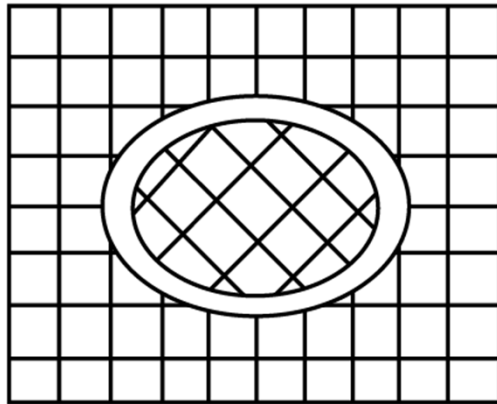
Influence of strain E (δ = lattice misfit) on the equilibrium shape of coherent precipitation

B. Incoherent Inclusions

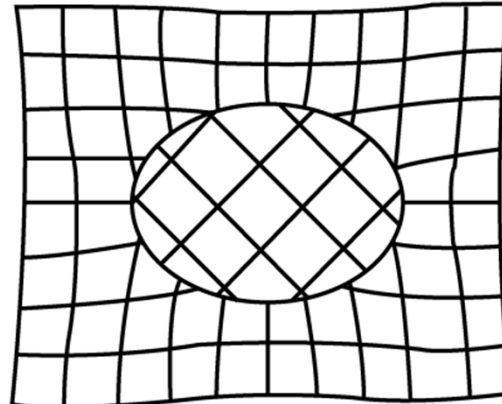
Lattice sites are not conserved. → no coherency strain, ΔG_s

But, misfit strain still arise if the inclusion is the wrong size.

δ (lattice misfit) → Δ (volume misfit)



(a)



(b)

$$\text{Volume Misfit } \Delta = \frac{\Delta V}{V}$$

Ex) coherent spherical inclusion: $\Delta=3\delta$

#of lattice sites within the hole is not preserved for incoherent inclusion (no lattice matching)

For spheroidal Inclusions $\frac{x^2}{a^2} + \frac{y^2}{b^2} + \frac{z^2}{c^2} = 1$

For Elliptical Inclusions $\frac{x^2}{a^2} + \frac{y^2}{a^2} + \frac{z^2}{c^2} = 1$

For a homogeneous incompressible inclusion in an isotropic matrix

등방성 기지내 균질 비압축성 개재물

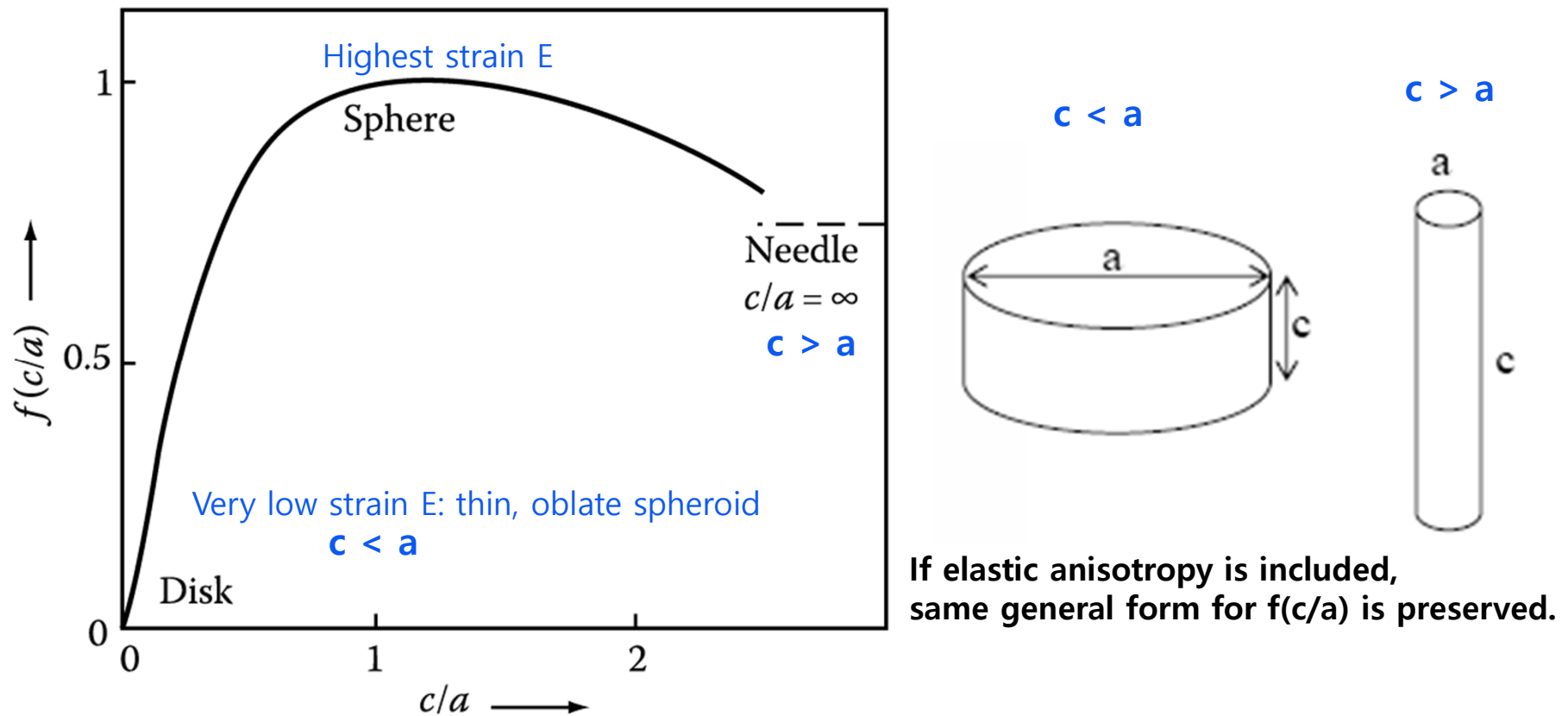
Nabarro Eq.

$$\Delta G_s = \frac{2}{3} \mu \Delta^2 \cdot V \cdot f(c/a)$$

μ : the shear modulus of the matrix

1) The elastic strain energy is proportional to the square of the volume misfit Δ^2 .

2) Shape effect for misfit strain $E \sim$ function $f(c/a)$



If elastic anisotropy is included, same general form for $f(c/a)$ is preserved.

Fig. 3. 50 The variation of misfit strain energy with ellipsoid shape, $f(c/a)$.

$$\Delta G_s = \frac{2}{3} \mu \Delta^2 \cdot V \cdot f(c/a) \quad \Delta = \frac{V_\beta - V_\alpha}{V_\alpha} \approx 3\delta \text{ for sphere}$$

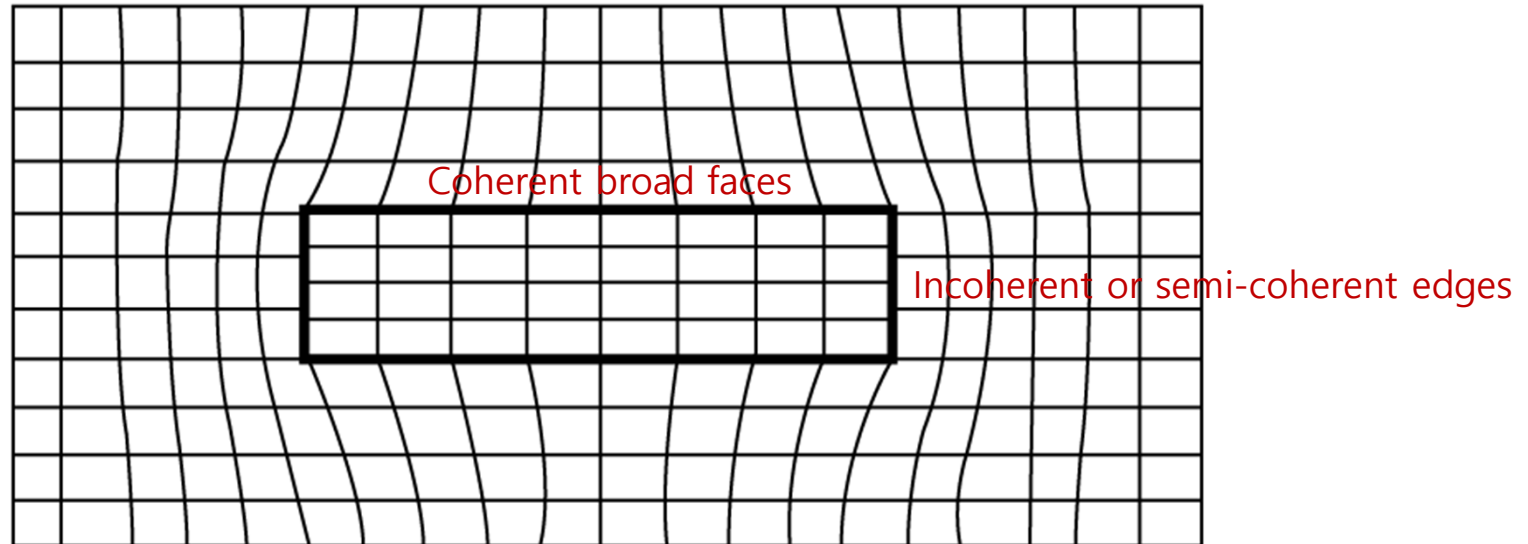
Elastic strain E Precipitate shape effect $\neq 3\delta$ for disc or needle

* Equil. Shape of an incoherent inclusion: an oblate spheroid with c/a value that balances the opposing effects of interfacial E and strain E

(here, $\Delta \sim$ small \rightarrow Interfacial E dominant \rightarrow roughly spherical inclusion)

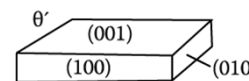
C. Plate-like precipitates

Misfit across the broad faces → large coherency strains parallel to the plate



In situ misfit across the broad faces increases with increasing plate thickness

- greater strains the matrix and higher shear stresses at the corners of the plates
- energetically favorable for the broad faces to become semi-coherent
- the precipitate behaves as **an incoherent inclusion with comparatively little misfit strain E , ex) θ' phase in Al-Cu alloy**



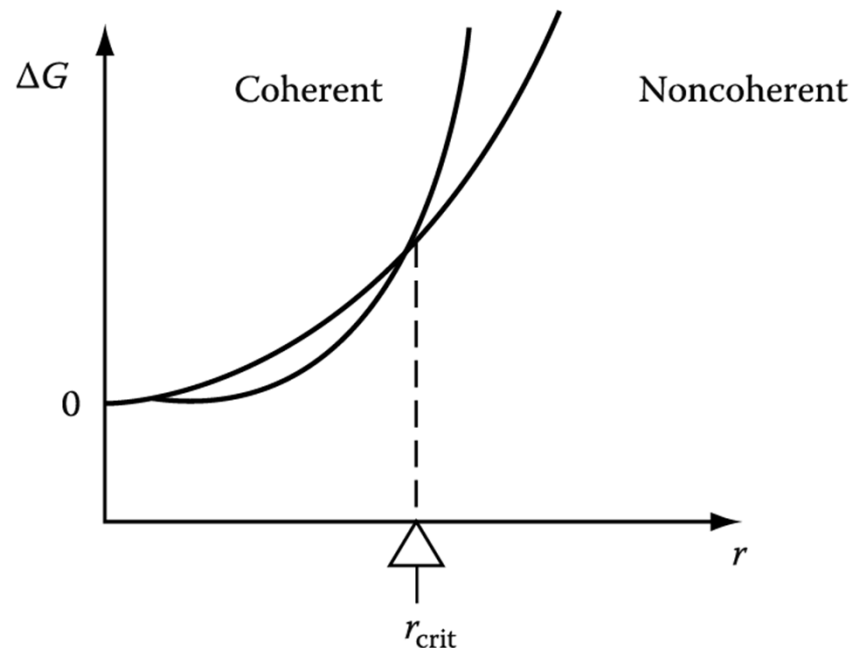
(001) Coherent or semicoherent

$\left. \begin{matrix} (100) \\ (010) \end{matrix} \right\}$ Not coherent

Q: Which state produces the lowest total E for a spherical precipitate?

“Coherency loss”

If a coherent precipitate grows, during aging for example, it should lose coherency when it exceeds r_{crit} .

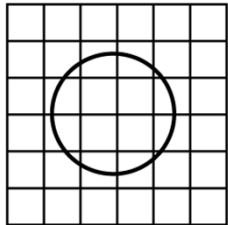


Coherency Loss

- Precipitates with coherent interfaces = low interfacial E + coherency strain E
- Precipitates with non-coherent interfaces = higher interfacial E

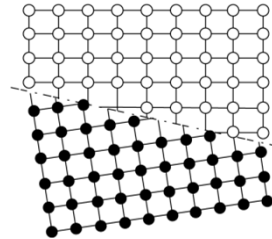
If a coherent precipitate grows, it should lose coherency to maintain minimum interfacial free E.

$$\Delta G(\text{coherent}) = 4\mu\delta^2 \cdot \frac{4}{3}\pi r^3 + 4\pi r^2 \cdot \gamma_{ch} \iff \Delta G(\text{non-coherent}) = 4\pi r^2 \cdot (\gamma_{ch} + \gamma_{st})$$



Coherency strain energy
Eq. 3.39

Chemical interfacial E



Chemical and structural interfacial E

$$\frac{4}{3}\pi r^3 (4\pi\mu\delta^2) + 4\pi r^2 (\gamma_{ch}) = 4\pi r^2 (\gamma_{st} + \gamma_{ch})$$

coherent

ΔG_s -relaxed

$$\therefore r_{crit} = \frac{3 \cdot \gamma_{st}}{4\mu\delta^2}$$

for small δ , $\gamma_{st} \propto \delta$
(semi-coherent interface)

$$\approx \frac{1}{\delta} \quad (\delta = (d_\beta - d_\alpha) / d_\alpha : \text{misfit})$$

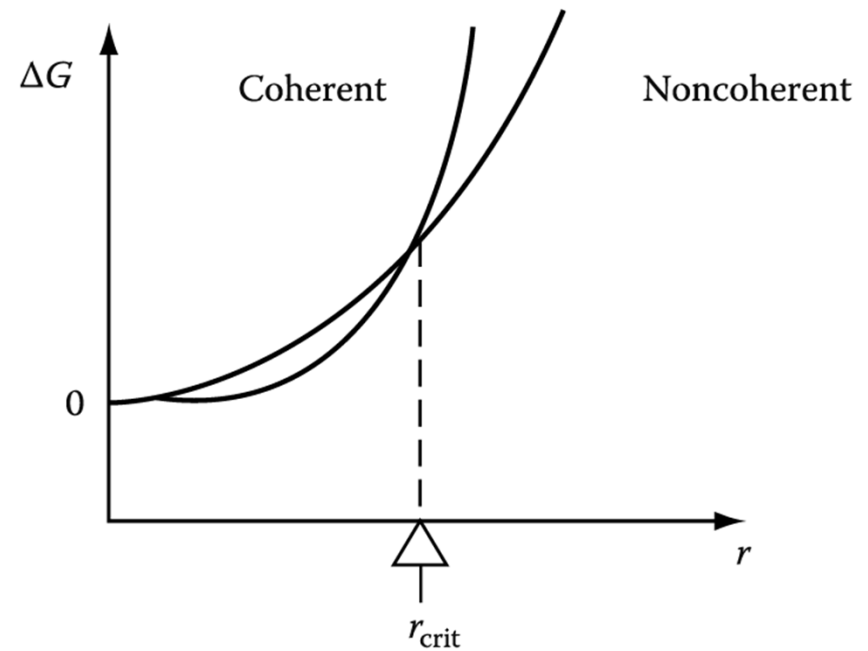


Fig. 3. 52 The total energy of matrix + precipitate vs. precipitate radius for spherical coherent and non-coherent (semicoherent or incoherent) precipitates.

If a coherent precipitate grows, during aging for example, it should lose coherency when it exceeds r_{crit} .

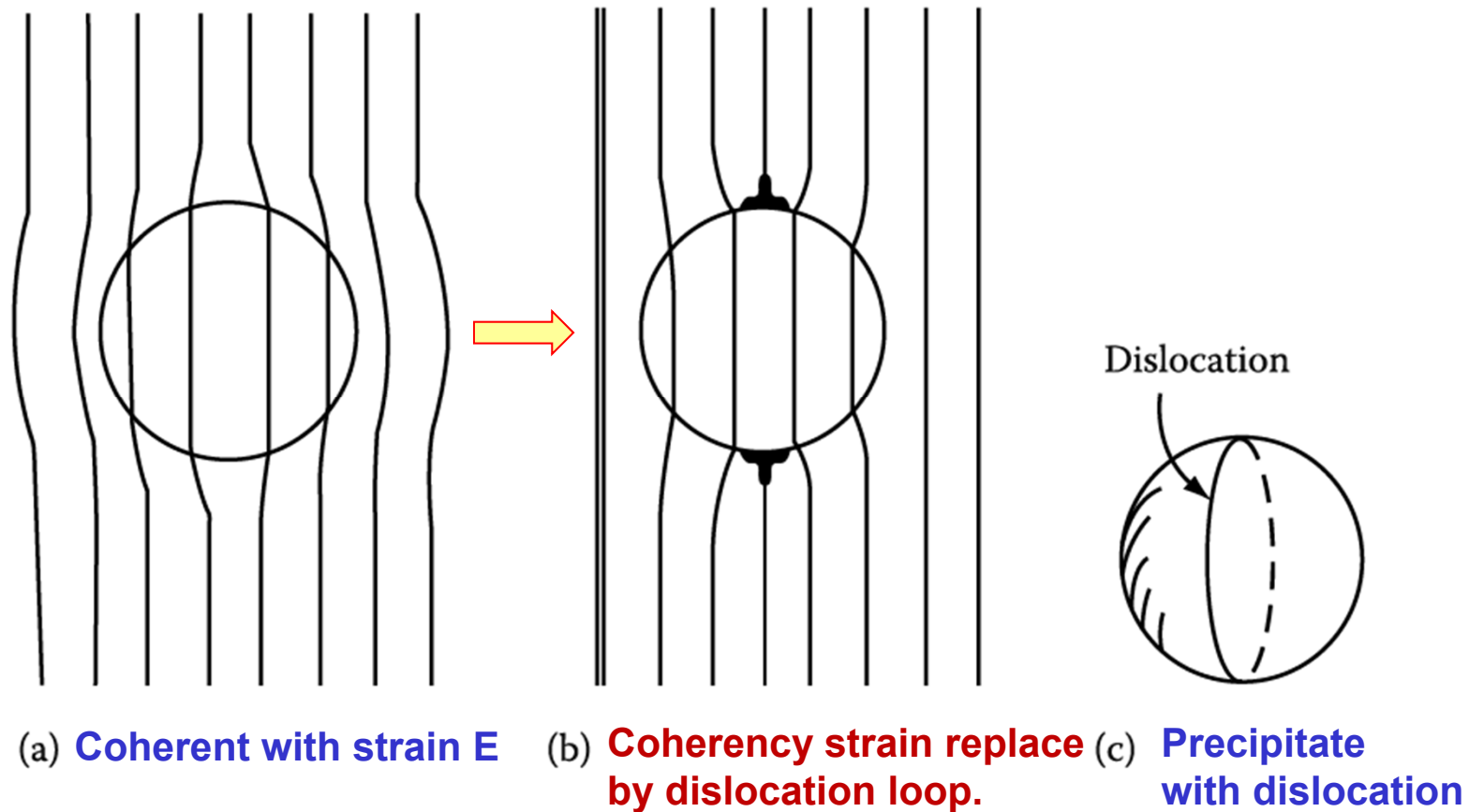


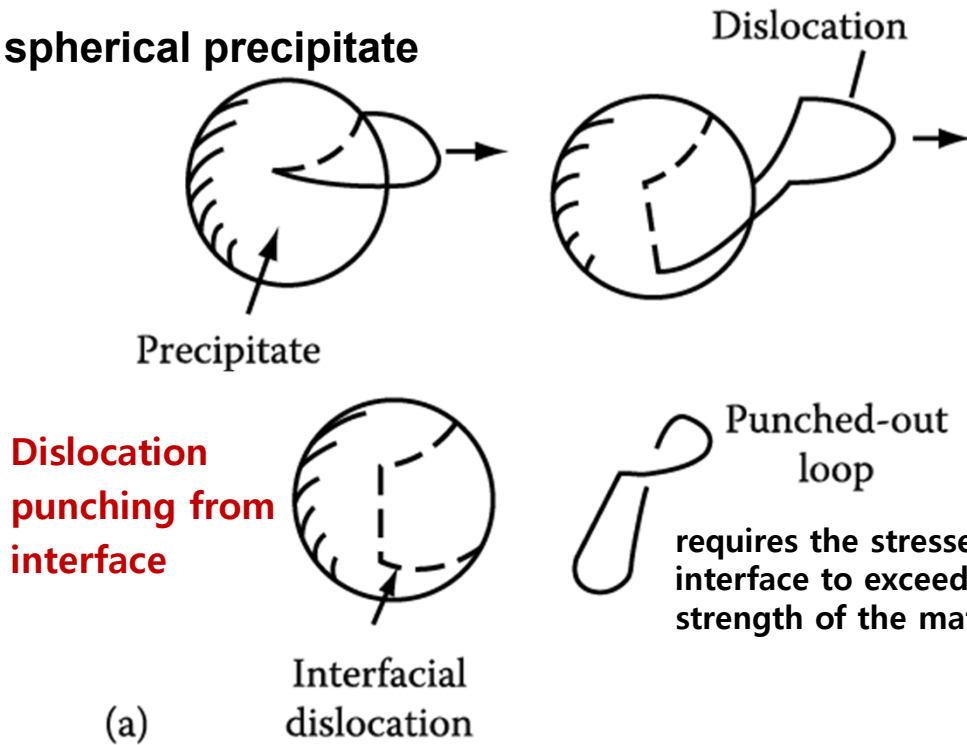
Fig. 3.53. Coherency loss for a spherical precipitate

In practice, this phenomena can be rather difficult to achieve.

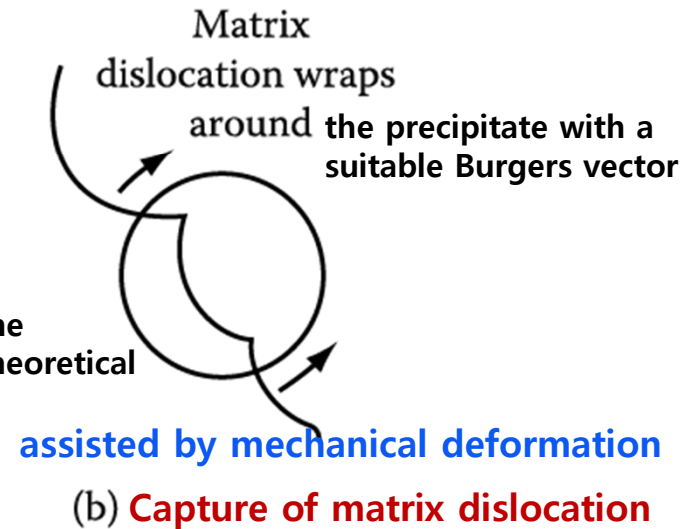
→ Coherent precipitates are often found with sizes much larger than r_{crit} .

“Mechanisms for coherency loss”: all require the precipitate to reach a larger size than r_{crit}

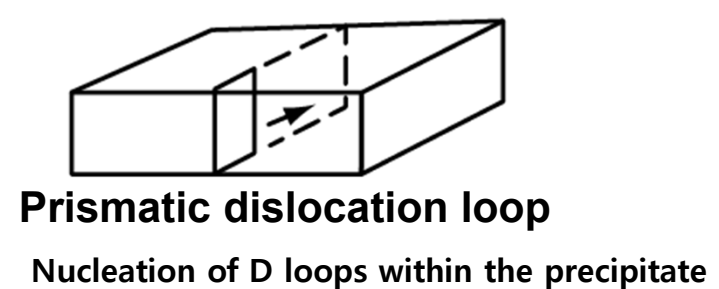
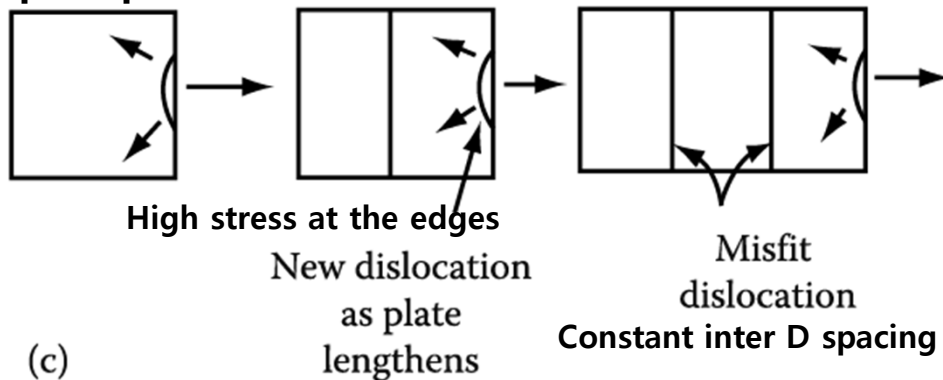
1) spherical precipitate



* Punching stress (P_s) \sim independent of size, but $P_s \propto$ constrained misfit, ϵ ($>\epsilon_{crit} \sim 0.05$), \rightarrow “precipitates with a smaller ϵ cannot lose coherency by (a), no matter how large.”



2) Plate precipitate



Nucleation of dislocation at the edge \rightarrow maintain a roughly constant inter-dislocation spacing during plate lengthening

(d) Vacancies can be attracted to coherent interfaces and ‘condense’ to form a prismatic dislocation loop which can expand across the precipitate

Contents for previous class

3.4 Interphase Interfaces in Solids

Interphase boundary - different two phases : **different crystal structure**
different composition

coherent,

Perfect atomic matching at interface

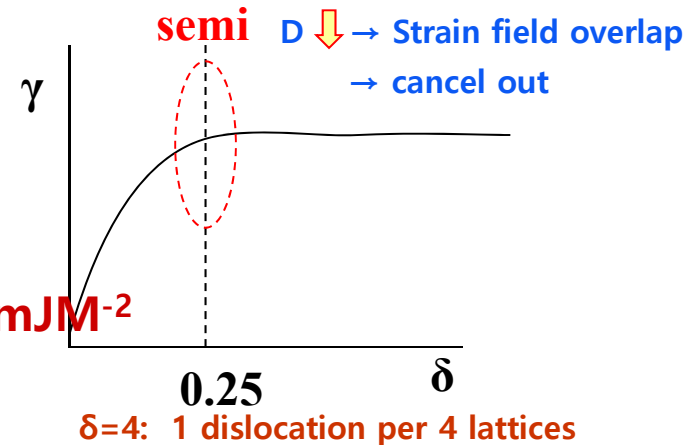
$$\gamma (\text{coherent}) = \gamma_{ch} \quad \gamma (\text{coherent}) \sim 200 \text{ mJM}^{-2}$$

semicoherent

$$\gamma(\text{semicoherent}) = \gamma_{ch} + \gamma_{st}$$

γ_{st} → due to structural distortions
caused by the misfit dislocations

$$\gamma(\text{semicoherent}) \sim 200 \sim 500 \text{ mJM}^{-2}$$



incoherent

1) $\delta > 0.25$ No possibility of good matching across the interface

2) different crystal structure (in general)

$$\gamma (\text{incoherent}) \sim 500 \sim 1000 \text{ mJM}^{-2}$$

Complex Semicoherent Interfaces

Nishiyama-Wasserman (N-W) Relationship

Kurdjumov-Sachs (K-S) Relationships

41

(The only difference between these two is a rotation in the closest-packed planes of 5.26° .)

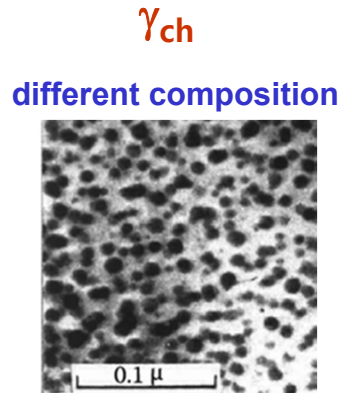
The degree of coherency can, however, be greatly increased if a macroscopically irrational interface is formed.

3.4 Interphase Interfaces in Solids

$$\sum A_i \gamma_i + \Delta G_S = \text{minimum}$$

Lowest total interfacial free energy
by optimizing the **shape of the precipitate** and **its orientation relationship**

Fully coherent precipitates



$\gamma_{ch} + \text{Lattice misfit}$ $\Rightarrow \gamma_{ch} + \text{Volume Misfit } \Delta = \frac{\Delta V}{V}$

Coherency strain energy Chemical and structural interfacial E

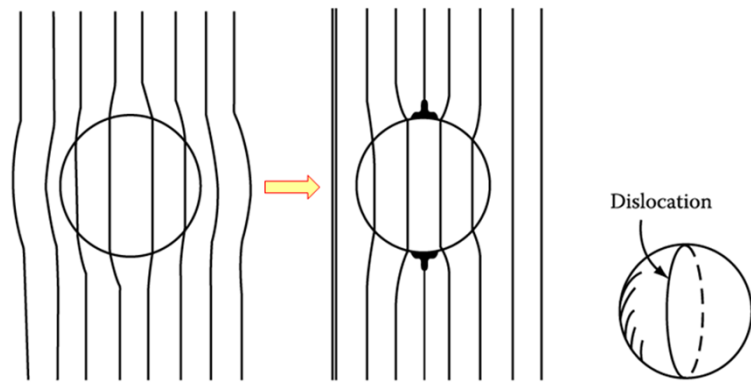
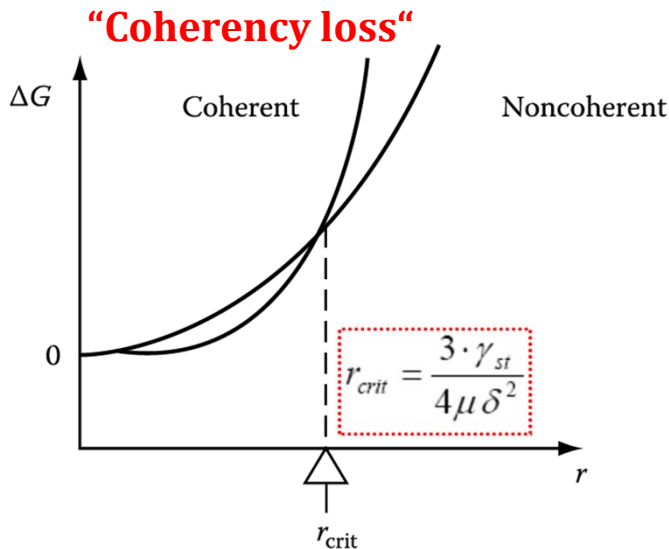
$\Delta G_S = 4\mu\delta^2 \cdot V$ (If $\nu=1/3$) $\leftrightarrow \Delta G_S = \frac{2}{3}\mu\Delta^2 \cdot V \cdot f(c/a)$

Fully coherent precipitates Incoherent inclusions

$$\Delta G(\text{coherent}) = 4\mu\delta^2 \cdot \frac{4}{3}\pi r^3 + 4\pi r^2 \cdot \gamma_{ch}$$

$\Delta G(\text{non-coherent}) = 4\pi r^2 \cdot (\gamma_{ch} + \gamma_{st})$

Incoherent inclusions



(a) Coherent with strain E (b) Coherency strain replace by dislocation loop. (c) Precipitate with dislocation

